ISSN: 2157-9423 Vol. 1, No. 2, October 2010

Scientific Research

Pharmacology and Pharmacy

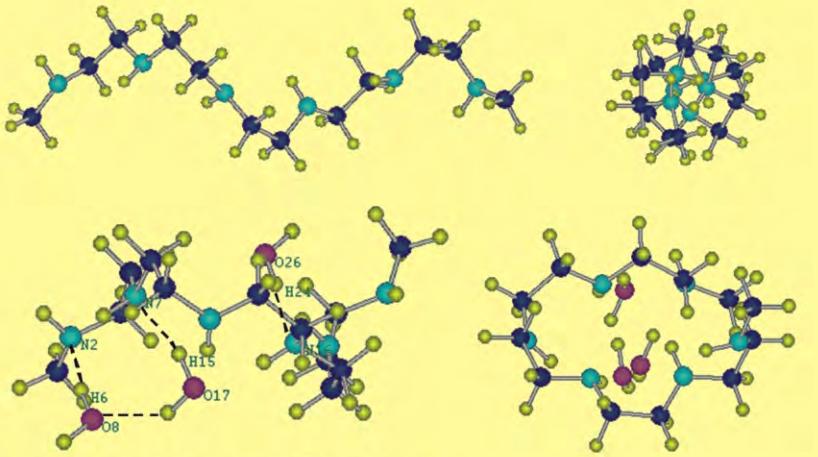

d_{N-H} (Å): N2-H6=1.90, N7-H15=1.94, N16-H24=1.90,
d_{N-O} (Å): N2-O8=2.86, N7-O17=2.89, N16-O26=2.87,
d_{O-O} (Å): O8-O17=2.80.

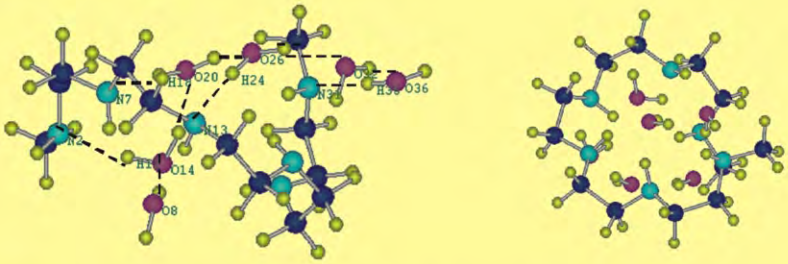

d_{N-H} (Å): N2-H12=2.00, N7-H18=1.93, N13-H24=1.99, N31-H35=1.83,
d_{N-O} (Å): N2-O14=2.95, N7-O20=2.89, N13-O26=2.95, N31-O36=2.79,
d_{O-O} (Å): O8-O14=2.76, O14-O20=2.71, O20-O26=2.71, O26-O32=2.75, O32-O36=2.76.

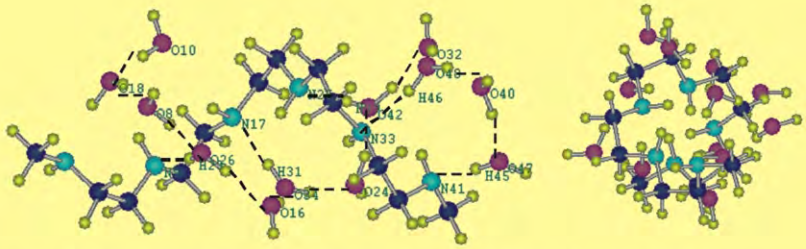

d_{N-H} (Å): N9-H23=1.99, N17-H31=1.94, N25-H39=1.98, N33-H46=2.00, N41-H45=1.79,
d_{N-O} (Å): N9-O26=2.94, N17-O34=2.91, N25-O42=2.94, N33-O48=2.94, N41-O47=2.77,
d_{O-O} (Å): O10-O18=2.69, O18-O8=2.71, O8-O26=2.62, O26-O16=2.74,O16-O34=2.61, O34-O24=2.71,
O24-O42=2.61, O42-O32=2.71, O32-O48=2.62, O48-O40=2.71, O40-O47=2.66.

ISSN: 2157-9423

www.scirp.org/journal/pp

Journal Editorial Board

ISSN: 2157-9423 (Print) ISSN: 2157-9431 (Online)

http://www.scirp.org/journal/pp

Editor-in-Chief

Editorial Board

Editorial Assistant

Guest Reivewer

Pharmacology & Pharmacy, **2010, 1, 39-74**
Published Online October 2010 in SciRes (http://www.SciRP.org/journal/pp/)

TABLE OF CONTENTS

Volume 1 Number 2 **October 2010**

Colchicine-Induced Rhabdomyolysis and Possible Amiodarone Interaction

C. B. Salem, J. Sakhri, N. Fathallah, B. Trimech, H. Hmouda, B. Kamel……39

Rational Drug Delineation: A Global Sensitivity Approach Based on Therapeutic Tolerability to Deviations in Execution

D. G. Gohore, F. Fenneteau, O. Barrière, J. Li, F. Nekka……42

Antioxidant Effect of Atorvastatin in Type 2 Diabetic Patients

N. R. Hadi, M. A. Abdelhussein, O. M. O. Alhamami, A. R. M. Rudha, E. Sabah……53

Structure Analysis for Hydrate Models of Ethyleneimine Oligomer by Quantum Chemical Calculation

M. Kobayashi, H. Sato……60

The Study of Influence of Silica and Polyethilene Glycols Organic-Inorganic Compounds on Free-Radical Processes *in Vitro*

O. G. Sitnikova, S. B. Nazarov, I. V. Shikhanova, A. V. Agafonov, J. A. Dyuzhev, I. G. Popova……69

The figure on the front cover is from the article published in Pharmacology & Pharmacy, 2010, Vol. 1, No. 2, pp. 60-68, by Minoru Kobayashi, Hisaya Sato.

Pharmacology & Pharmacy

Journal Information

SUBSCRIPTIONS

The *Pharmacology & Pharmacy* (Online at Scientific Research Publishing, www.SciRP.org) is published quarterly by Scientific Research Publishing, Inc., USA.

Subscription rates:

Print: $50 per copy.
To subscribe, please contact Journals Subscriptions Department, E-mail: sub@scirp.org

SERVICES

Advertisements
Advertisement Sales Department, E-mail: service@scirp.org

Reprints (minimum quantity 100 copies)
Reprints Co-ordinator, Scientific Research Publishing, Inc., USA.
E-mail: sub@scirp.org

COPYRIGHT

PRODUCTION INFORMATION

For manuscripts that have been accepted for publication, please contact:
E-mail: pp@scirp.org

Pharmacology & Pharmacy, **2010, 1, 39-41**
doi:10.4236/pp.2010.12006 Published Online October 2010 (http://www.SciRP.org/journal/pp)

Colchicine-Induced Rhabdomyolysis and Possible Amiodarone Interaction

——Colchicine-Induced Rhabdomyolysis

Chaker Ben Salem[1], Jaballah Sakhri[2], Neila Fathallah[1], Besma Trimech[3], Houssem Hmouda[4], Bouraoui Kamel[1]

[1]Department of Clinical Pharmacology, Faculty of Medicine of Sousse, Sousse, Tunisia; [2]Department of Surgery, Farhat Hached Hospital, Sousse, Tunisia; [3]Department of Cardiology, Farhat Hached Hospital, Sousse, Tunisia; [4]Medical Intensive Care Unit, Sahloul Hospital, Sousse, Tunisia.
Email: bensalem.c@gmail.com

Received August 10th, 2010; revised August 25th, 2010; accepted September 5th, 2010.

ABSTRACT

***Objective*:** *To report a case of drug interaction leading to rhabdomyolysis.* ***Case Summary*:** *A 65-year old woman suffering from chronic atrial fibrillation was treated with amiodarone and acenocoumarol. Two weeks after administration of conventional dosage of colchicine for pericarditis, the patient developed rhabdomyolysis. colchicine-induced rhabdomyolysis was suspected. Colchicine was stopped and the patient underwent supportive therapy. Clinical symptoms improved rapidly.* ***Discussion*:** *Colchicine-induced neuromuscular toxicity and rhabdomyolysis have been reported with chronic treatment in therapeutic doses. Concomitant use of several drugs with colchicine may potentiate the development of myopathy. In our case, a co-administration of colchicine, a well known substrate of cytochrome P450 3A4 and P-glycoprotein, and amiodarone had possibly precipitated rhabdomyolysis. Amiodarone may increase colchicine toxicity by a dual mechanism. Amiodarone inhibits P-glycoprotein which may theoretically result in increased intracellular colchicine concentrations and decreased hepatic and renal excretion of the drug.* ***Conclusion*:** *Amiodarone may potentiate the development of colchicine-induced rhabdomyolysis.*

***Keywords*:** *Colchicine, Rhabdomyolysis, Amiodarone, Interaction*

1. Introduction

Colchicine is an anti-inflammatory drug widely used in the treatment of a large panel of inflammatory diseases and particularly gout. Colchicine may induce many side effects, principally gastrointestinal adverse effects including abdominal pain, vomiting, and diarrhea. It may cause much more severe reactions such as bone marrow depression, myoneuropathy and myopathy. Rhabdomyolysis is a rare and lifethreatening adverse effect of colchicine. We report a case of rhabdomyolysis possibly induced by colchicine and concomitant use of amiodarone.

2. Case Report

A 65-year old woman suffering from chronic atrial fibrillation treated with amiodarone (200 mg daily; 5 days per week) and acenocoumarol (0.25 mg daily). She also received captopril (25 mg daily); furosemide (40 mg daily); molsidomine (75 mg daily) and spironolactone (50 mg daily) for ischemic cardiomyopathy. Colchicine therapy (1 mg daily) has been started two weeks before admission for pericarditis. She was admitted to cardiology department for management of over-anticoagulation by acenocoumarol manifested by epistaxis and melena. On admission, the patient was afebrile. The relevant physical findings were atrial fibrillation without signs of acute decompensated heart failure. The patient also reported myalgia and diffuse muscle weakness. Both sensation and coordination were intact. She had no recent viral illness and she denied any change from her normal level of activity. No alcohol ingestion, illicit drugs, or trauma were present. There were no signs of liver insufficiency or for thyroid disease.

Laboratory tests revealed the following: international normalized ratio (INR) at 6.5 UI/l, creatine kinase (CK) at 5780 UI/L (normal range: 40-150 U/L) and aldolase at 3700 UI/L (normal range: 06-16 UI/L). Blood cell count, renal function, liver enzymes, potassium and troponin

serum levels were within normal range. Viral tests did not disclose any viral infection. Based on clinical and biological findings, colchicine-induced rhabdomyolysis was suspected. Muscle biopsy was not performed because of high INR. Colchicine was stopped and the patient underwent supportive therapy. The other drugs were given continuously. Clinical symptoms improved rapidly with a progressive decrease in CK and aldolase levels. Few days later, CK level decreased to 384 UI/L, and aldolase level to 100 UI/L. However, the patient died from ventricular fibrillation.

3. Discussion

Colchicine-induced neuromuscular toxicity and rhabdomyolysis have been reported with chronic treatment in therapeutic doses. Patients with renal dysfunction and elderly patients, even those with normal renal and hepatic function, are at increased risk. Concomitant use of atorvastatin, simvastatin, pravastatin, lovastatin, fluvastatin, gemfibrozil, fenofibrate, fenofibric acid, or benzafibrate (themselves associated with myotoxicity) or cyclosporine may potentiate the development of myopathy [1-4].

Colchicine is a well known substrate of cytochrome P450 3A4 (CYP3A4) in the liver and gastrointestinal (GI) tract, along with P-glycoprotein efflux pumps (P-gp) in the GI tract. Potent CYP3A4 inhibitors such as clarithromycin, cyclosporine, diltiazem, erythromycin, grapefruit juice, itraconazole, ketoconazole, and verapamil may increase colchicine levels and the subsequent risk of toxicity [5]. Many CYP3A4 inhibitors also inhibit P-gp, which could further increase this effect.

Amiodarone is a well known CYP3A4 and P-gp inhibitor [6,7]. This inhibition is primarily because of its active metabolite, desethylamiodarone, which noncompetitively inhibits 3A4. Thus, Amiodarone co-administration may increase colchicine toxicity by a dual mechanism. Amiodarone inhibits P-glycoprotein which may theoretically result in increased intracellular colchicine concentrations and decreased hepatic and renal excretion of the drug. Amiodarone may also interact with CYP3A4 to decrease the hepatic elimination of colchicine. Several drugs increase the potential for colchicine toxicity via dual modulation of CYP3A4 and P-gp [8]. These include the macrolide antibiotics erythromycin and clarithro-mycin, and the statins (lovastatin, simvastatin, atorvastatin).

Based on the Naranjo probability scale, it is probable that colchicine caused this patient's rhabdomyolysis, and the Horn drug interaction probability scale indicates a possible interaction between colchicine and amiodarone [9,10]. Our case highlights a previously unknown drug interaction. Rhabdomyolysis developed few days after starting standard dose of colchicine in a patient without renal insufficiency.

The FDA recently reviewed the safety of oral colchicine [5]. New drug interactions have been identified with this agent. Oral colchicine was linked to 169 cases of fatal toxicity. One-hundred seventeen cases occured in patients taking therapeutic doses, and over half of these 117 cases involved concomitant use of clarithromycin.

Colchicine-induced rhabdomyolysis is an acute life-threatening disease. The main goal of treatment is to stop muscle destruction. The rapid withdrawal of the drug is crucial. Once colchicine is stopped, the symptoms generally resolve within 1 week to several months [5].

The exact mechanism of colchicine-induced myoneuropathy is still unclear. Colchicine affects microtubular cell function, it may cause disruption of axonal transport and organelle trafficking in both nerve and muscle cells at the bases of clinical deficits. Electromyography shows fibrillations, positive sharp waves, and low-amplitude distal motor and sensory potentials. If performed, muscle biopsy shows characteristic vacuolar myopathy with no associated necrosis. In another side, the over-anticoagulation by acenocoumarol manifested by epistaxis and melena (reason for admission) may be precipitated by amiodarone co-administration. The potentiation of acenocoumarol anticoagulant effect by amiodarone is well established. In our patient, concomitant medications such as captopril, furosemide, molsidomine and spironolactone seem to not interfere with colchicine. These drugs are not known to be CYP3A4 or P-gp inhibitor.

At present, colchicine has been recommended by the 2004 European guidelines on the management of pericardial diseases for acute (class IIa) and recurrent pericarditis (class I), but its use is still unlabeled and informed consent is required for prescription [11].

The indication of treatment with colchicine should be carefully considered especially in poly-medicated patients. Patients should be informed that muscle pain or weakness may occur with colchicine alone or when it is used with certain other drugs such as amiodarone. Patients should be educated to report symptoms of myopathy immediately to physicians who may decide to discontinue colchicine treatment.

4. Conclusions

Our case suggests a possible interaction between colchicine and amiodarone that appears theoretically possible but not yet confirmed. We recommend that further *in vivo* studies be completed to definitively identify the mechanism of the interaction amiodarone-colchicine.

REFERENCES

[1] W. C. Hsu, W. H. Chen, M. T. Chang and H. C. Chiu,

"Colchicine-Induced Acute Myopathy in a Patient with Concomitant Use of Simvastatin," *Clinical Neuropharmacology*, Vol. 25, No. 5, September-October 2002, pp.266-8.

[2] G. Alayli, K. Cengiz, F. Cantürk, D. Durmus, Y. Akyol, E.B. Menekse, "Acute Myopathy in a Patient with Concomitant Use of Pravastatin and Colchicines" *Annals of Pharmacotherapy*, Vol. 39, No. 5, July-August 2005, pp. 1358-1361.

[3] I. Akdag, A. Ersoy, S. Kahvecioglu, M. Gullulu and K. Dilek, "Acute Colchicine Intoxication during Clarithromycin Administration in Patients with Chronic Renal Failure" *Journal of Nephrology*, Vol. 19, No. 4, July-August 2006, pp. 515-517.

[4] I. F. Hung, A. K. Wu, V. C. Cheng, B. S. Tang, K. W. To, C. K. Yeung, P. C. Woo, S. K. Lau, B. M. Cheung and K. Y. Yuen, "Fatal Interaction between Clarithromycin and Colchicine in Patients with Renal Insufficiency: A Retrospective Study," *Clinical Infectious Diseases*, Vol. 41, No. 3, August 2005, pp. 291-300.

[5] http://www.accessdata.fda.gov/drugsatfda_docs/label/2009/022351lbl.pdf

[6] M. Katoh, M. Nakajima, H. Yamazaki and H. T. Yokoi, "Inhibitory Effects of CYP3A4 Substrates and their Metabolites on P-Glycoprotein-Mediated Transport," *European Journal of Pharmaceutical Sciences*, Vol. 12, No. 4, February 2001, pp. 505-513.

[7] W. Yamreudeewong, M. DeBisschop, L. G. Martin, D. L Lower, "Potentially Significant Drug Interactions of Class III Antiarrhythmic Drugs," *Drug Safety*, Vol. 26, No. 6, June 2003, pp. 421-438.

[8] E. Niel and J. M. Scherrmann, "Colchicine Today," *Joint Bone Spine*, Vol. 73, No. 6, 2006, pp. 672-678.

[9] C. A. Naranjo, U. Busto, E. M. Sellers, P. Sandor, I. Ruiz, E. A. Roberts, E. Janecek, C. Domecq and D. J. Greenblatt, "A Method for Estimating the Probability of Adverse Drug Reactions," Clinical Pharmacology Therapeutics, Vol. 30, No. 2, August 1981, pp. 239-245.

[10] J. R. Horn, P. D. Hansten and L. N. Chan, "Proposal for a New Tool to Evaluate Drug Interaction Cases," *Annals of Pharmacotherapy*, Vol. 41, No. 4, April 2007, pp. 674-680.

[11] M. Imazio, R. Trinchero and Y. Adler, "Colchicine for the Treatment of Pericarditis," *Future Cardiology*, Vol. 4, No. 6, November 2008, pp. 599-607.

Pharmacology & Pharmacy, **2010, 1, 42-52**
doi:10.4236/pp.2010.12007 Published Online October 2010 (http://www.SciRP.org/journal/pp)

Rational Drug Delineation: A Global Sensitivity Approach Based on Therapeutic Tolerability to Deviations in Execution

Denis Goue Gohore[1], Frédérique Fenneteau[2], Olivier Barrière[1], Jun Li[1,3], Fahima Nekka[1,3]

[1]Faculté de Pharmacie, Université de Montréal, Montréal, Canada; [2]Pharsight, A certara company, Montréal, Canada; [3]Centre de Recherches Mathématiques, Université de Montréal, Montréal, Canada.
Email: fahima.nekka@umontreal.ca

Received August 25th, 2010; revised September 10th, 2010; accepted September 20th, 2010.

ABSTRACT

Noncompliance to therapeutic regimen is a real public health problem with tremendous socioeconomic consequences. Instead of direct intervention to patients, which can add extra burden to the already overloaded health system, alternative strategies oriented to drugs' own properties turns to be more appealing. The aim of this study was establish a rational way to delineate drugs in terms of their "forgiveness", based on drugs PK/PD properties. A global sensitivity analysis has been performed to identify the most sensitive parameters to dose omissions. A Comparative Drug Forgiveness Index (*CDFI*), *to rank the drugs in terms of their tolerability to non compliance, has been proposed. The index was applied to a number of calcium channel blockers, namely benidipine, nivaldipine, manidipine and felodipine. Using the calculation, benedipine and manidipine showed the best performance among those considered. This result is in accordance with what has been previously reported. The classification method developed here proved to be a powerful quantitative way to delineate drugs in terms of their forgiveness and provides a complementary decision rule for clinical and experimental studies.*

Keywords: *Compliance*, *Drug Forgiveness*, *Global Sensitivity Analysis*, *Comparative Drug Forgiveness Index*, *Monte-Carlo*

1. Introduction

Compliance has been referred to as a dimensionless, blanket concept encompassing the extent to which patients' drug dosing histories conform, or not, to prescribed drug dosing regimen, in terms of both persistence and quality of execution compliance [1]. As a human behaviour, the patient compliance has an intrinsic complex nature which is in part responsible for the gap observed between the abundance of descriptive research and the shortage of quantitative tools. The tendency of the public health care system towards reducing hospitalization costs along with the increase in more powerful self-administered drugs, call for efficient evaluation methods to capture the multidimensional character of compliance and evaluate its clinical impact [2]. When dealing with adherence-related problems, the most spread practice is to enhance patients' adherence through intervention programs. This interactive approach, when successful, has proved to be beneficial for all the involved parts, including the patient, health care givers as well as the pharmaceutical industry. However, this individualized approach can easily become a burden for the health system, with too many aspects involved in the management of the patient's adherence [2] Recent efforts are more focused on the development of objective ways for compliance control and improvement. Remarkable advances in this important therapeutic-related area have been achieved, as reported in the review paper of Düsing [3]. In fact, work on compliance can be viewed from different angles. One can address the quantitative relationship of drug intake with its therapeutic outcomes, or alternatively looks for solutions to reduce the negative impact of poor compliance. The underline of the former aspect relies on the direct link of compliance to therapy. The latter however considers minimizing the impact of poor compliance upstream, putting emphasis on drugs and their pharmacokinetic and pharmacodynamic (PK/

PD) properties, with the intention to compare drug tolerability to changes in drug execution. This has led to the concept of "drug forgiveness" which is formally defined as the drugs post-dose duration of action minus the prescribed dosing interval [4]. An early molecule screening procedure, targeted to prioritize flexible drugs in terms of their forgiveness, is important in drug research and development for enhancement of the quality of therapy and reduction in costs. Indeed, this procedure could add a (market) value to those drugs having the least sensitive profile to irregular drug intake. The implication of compliance in pharmaceutical value has been previously highlighted by Urquhart [4].

Modeling and simulation approaches have become an integral part of the biopharmaceutical research, encompassing all aspects of the critical path of drug development and evaluation, including adherence studies. Many papers have focused on modeling human behaviour in relation to treatment recommendations [5-11]. Others have tried to understand the complex relationship between adherence, exposure and therapeutic response to a treatment [8,12-14]. In this paper, a modeling and simulation strategy based on sensitivity analysis to classify drugs according to their degrees of forgiveness was developed. It is based on the control of uncertainties in drug-related information that aims at ranking drugs in terms of their tolerance to dose omissions. The design of this classification procedure uses a recently developed global sensitivity analysis strategy, involving the Partial Ranked Correlation Coefficient (PRCC) method [15-19]. In this method, a family of calcium channel blockers was used in which four of them were chosen as drug models exhibiting a large spectrum of PK/PD properties, namely benedipine, nivaldipine, manidipine and felodipine.

This paper is organized as follows. In Materials and Methods, we describe our modeling approach and the global sensitivity analysis that will be used here and we define the comparative drug forgiveness index and explain how it can be used to classify drugs in terms of drug forgiveness. In Results, we present the results of drug classification in terms of their PK and PD properties and analyse its robustness for various compliance models.

2. Materials and Methods

2.1. The General Approach

In this study, the approach relied on building a combined model composed of three sub-models describing one-by one and in a chronological way, drug intake, drug disposition through the pharmacokinetics and the relationship between pharmacokinetics and pharmacodynamics as shown in **Figure 1**. The sensitivity analysis for the model parameters that were likely to carry out the most information on therapeutic effect in response to dose omissions for different dosing regimens was performed. For this, two clinical compliance indices that translate the impact of patient compliance in therapeutic outcomes were introduced. A global sensitivity analysis was performed to determine the coefficient of correlation (CC) between the PK and PD parameters for a given compliance index. These CCs were then converted into transitory scores that were used to estimate Comparative Drug Forgiveness Index (CDFI) that were used to classify drugs having similar pharmacological mechanisms. As an application of this approach, four long acting calcium channel blockers with various compliance situations were studied. Compliance scenarios were generated through three modeling approaches, namely, 1) Markov chain, 2) fixed percentages of taken doses and 3) different cases of drug holidays.

2.2. Model Components

2.2.1. Compliance Model

Several modeling approaches were used to simulate patients' drug intake. They include Markov Chain compliance model, drug holidays compliance model and Fixed

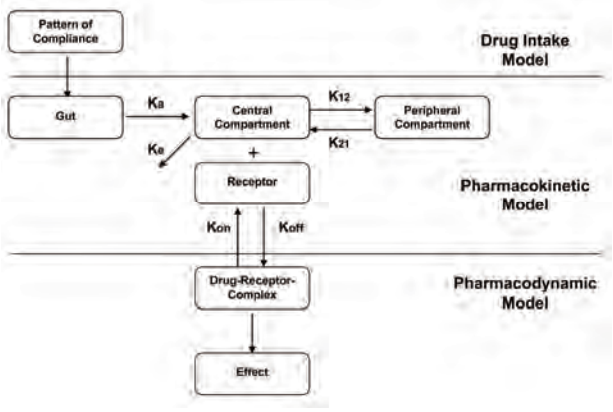

Figure 1. Conceptual model describing the three linked drug intake-PK-PD components, with the receptor-binding models describing the drug effect. $K_a\left(h^{-1}\right)$ is the absorption rate constant, $K_{12}\left(h^{-1}\right)$ and $K_{21}\left(h^{-1}\right)$ are the transfer rate constants from the central compartment to the peripheral compartment, and from the peripheral compartment to the central compartment, respectively; $K_e\left(h^{-1}\right)$ is the constant of elimination of drug from the central compartment, $K_{on}\left((ng\times h)^{-1}\right)$ is the second-order association rate constant and $K_{off}\left(h^{-1}\right)$ is the first-order dissociation rate constant.

percentage of taken doses compliance model. The Markov chain-based approach is the most reported one that is used to simulate compliance from real data [20].

2.2.1.1. Markov Chain Compliance Model

Markov chain is a mathematical tool used to predict future states from the current ones. In the context of compliance, it was assumed that there are three possible dose states at nominal times: omitted dose (0), one taken dose (1) or a double dose (2). Transitions between these states, from one nominal time to the next, were represented by a 3 × 3 transition matrix **P**, with each (*i*,*j*) element, noted p_{ij}, corresponding to the transition probability from dose state *i* to dose state *j*. Hence, if we use a 3-dimensional vector $\pi = (p_0, p_1, p_2)$, where p_i are probabilities for the dose states *i*, *i* = 0, 1, 2 with $p_0 + p_1 + p_2 = 1$ to note the current state, then the next dose state probabilities are expressed by:

$$\pi \mathbf{P} = (p_0, p_1, p_2) \begin{bmatrix} p_{00} & p_{01} & p_{02} \\ p_{10} & p_{11} & p_{12} \\ p_{20} & p_{21} & p_{22} \end{bmatrix}. \quad (1)$$

In this study, transition matrix estimated by Sun et al. from data collected from 177 patients following an HIV clinical trial study was used. [21]. This matrix is:

$$\mathbf{P} = \begin{bmatrix} 0.23 & 0.58 & 0.19 \\ 0.12 & 0.81 & 0.07 \\ 0.14 & 0.75 & 0.11 \end{bmatrix}. \quad (2)$$

To mimic realistic compliance scenarios, dosing intervals with normal distributions are used, where average dosing intervals and standard deviation are set to μ = 24 h and σ = 12 h, respectively. Using the approach described in [6], the generated negative values are truncated and replaced with an arbitrary chosen small time length (0.01 h in our case) and are assigned to double doses. A typical dosing history is illustrated in **Figure 2**.

2.2.1.2. Drug Holidays Compliance Model

'Drug holidays' have been proved to be relevant to therapeutic outcomes. Defined as drug omissions over three successive days or more [9], they are reported to occur during weekends and in special events such as travel periods.

2.2.1.3. Compliance Model with Fixed Percentages of Taken Doses

The percentage of taken doses is the traditional cut-off used to classify patient compliance. It is commonly accepted that a patient who has taken at least 80% of prescribed doses is a 'perfect' compliant.

2.2.2. Pharmacokinetic Model

A two-compartmental PK model with first-order absorption and elimination for the calcium channel blockers was considered in the disposition model [22-24]. The disposition model was then linked to the compliance model through the gastro-intestinal tract as illustrated in **Figure 1**. The PK model was given by the following system of equations:

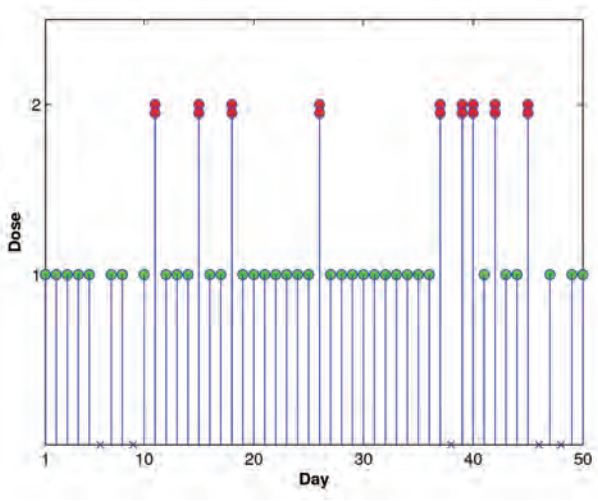

Figure 2. Illustrative example of dosing history. A single circle represents one taken dose, a double circle is for a double dose while a cross symbol is for an omitted dose.

$$\frac{dA_D}{dt} = Q - K_a \times A_D \quad (3)$$

$$\frac{dC_1}{dt} = \frac{K_a \times F \times A_D}{V_1} + \frac{K_{21} \times C_2 \times V_2}{V_1} - (K_e + K_{12}) \times C_1 \quad (4)$$

$$\frac{dC_2}{dt} = \frac{K_{12} \times C_1 \times V_1}{V_2} - K_{21} \times C_2 \quad (5)$$

where A_D (mg) was the absorbable amount of drug in the gastro-intestinal tract, *Q*(mg) was a time-dependant function of drug intake determined by compliance model , C_1 (mg/L) and C_2 (mg/L) were the central and peripheral concentrations, respectively, V_1 (L/kg) and V_2 (L/kg) were the apparent central and peripheral volumes of distribution, respectively. The other parameters were as in **Figure 1**. For sake of simplicity, bioavailability *F* was assumed to be 1.

2.2.3. PK/PD Model

2.2.3.1. Drug Class

Calcium channel antagonists are largely used for the management of various cardiovascular diseases including hypertension. It has been reported that there is a direct link between blood pressure and compliance to these drugs, where over 37% of hypertensive patients that undergo treatment, are stated non compliant [25].

2.2.3.2. Pharmacodynamic Model

The calcium channel blockers bind to calcium channels to limit the entry of calcium into the vascular and cardiac smooth muscles thus preventing muscle contractility. The intensity and duration of their action depend on their ability to dissociate at the target site. The indirect PK/PD model to characterize the effect of these drugs was used [22]. The effect $E(mHg)$ can be modeled as:

$$\frac{dE}{dt} = K_{on} \times \left(E_{\max} - E\right) - K_{off} \times E \qquad (6)$$

where $E_{\max}\left(mHg\right)$, K_{on} and K_{off} are the maximum effect, the association and dissociation rate constants, respectively.

2.3. Sensitivity Analysis of PK/PD Parameters

A global sensitivity analysis (GSA) of the combined model was applied to identify input parameters suspected to have determinant role on compliance indices under investigation. GSA is a probabilistic approach used to determine the sensitivity of the model outcomes to the variation of input parameters [26]. Using this approach, possible input parameter values were simulated and statistically analysed according to their distribution functions and possible correlations. GSA has recently been introduced to analyse the physiological based pharmacokinetic models [15,16].

The following terms were used in this work: the 'input parameter X_i' refers to one of the involved pharmacokinetic and pharmacodynamic parameters, and the 'output variable Y_j' to the model response.

2.4. Input Parameters

Nine parameters were investigated using GSA, namely: K_a, K_e K_{12}, K_{21}, V_1, V_2, K_{on}, K_{off} and $E_{\max}$. Based on the statistical description of input parameters for calcium channel inhibitors given in **Table 1** [22,27,28] Monte Carlo approach was used to generate a large number (N = 1000) of drugs, each having a specific vector composed of m = 9 input parameters (*i.e.*, a matrix of $m \times 1000$). These input parameters were used to generate the corresponding output parameters.

2.5. Output Parameters

Two important compliance indices relevant to anti-hypertensive therapy were chosen:

2.5.1. Number of Subtherapeutic Days (SD)

A patient was considered to have subtherapeutic plasma drug concentrations if the systolic blood pressure deviated by ΔE = 20% from the expected value if the patient was a perfect compliant. Using this well accepted clinical criterion [32], the number of SD following the calculation of ΔE for different compliance scenarios and input parameters was estimated. A higher SD indicates that the treatment success can be jeopardized.

Table 1. Statistical description of input parameters assumed to be log-normally distributed.

Parameters	Mean	Std	IC
$K_a\left(h^{-1}\right)$	0.80	0.37	0.30-3.20
$K_e\left(h^{-1}\right)$	0.36	0.13	0.10-1.20
$K_{12}\left(h^{-1}\right)$	0.14	0.12	0.02-1.00
$K_{21}\left(h^{-1}\right)$	0.10	0.10	0.008-0.82
$V_1\left(L\right)$	992.20	550.90	359.10-2,739
$V_2\left(L\right)$	5,758	3,770	2,788-18,563
$E_{max}\left(mHg\right)$	27.00	8.25	15.00-48.00
$K_{on}\left(ng.h^{-1}\right)$	0.70	0.90	0.05-3.00
$K_{off}\left(h^{-1}\right)$	0.36	0.50	0.01-5.00

2.5.2. Smoothness Index (SI)

SI is used to assess the fluctuation in blood pressure driven by the drug or treatment regimen. Clinically, this index indicates the homogeneity of blood pressure reduction induced by antihypertensive drug treatment over the 24 hours. A large variation in blood pressure (low SI) is likely to trigger organ damage, in comparison to a higher SI that indicates a smooth blood pressure [29-34]. Hence, an SI decrease can raise therapeutic concerns.

The smoothness index was obtained as:

$$SI = \frac{m_{DH}}{\sigma_{DH}} \qquad (7)$$

where mDH and σDH are the mean and standard deviation of systolic blood pressure calculated for a same individual, respectively.

2.6. Input-Output Correlation

In order to identify the important parameters and quantify their influence on model outcomes, the correlation (CC), rank correlation (RCC), partial correlation (PCC) or partial rank correlation (PRCC) coefficients were calculated according to the linearity or monotonicity properties of the input-output relationship, as well as to the correlation between input parameters [16]. In this study, nonlinear but monotonous relationships were observed between some input and output parameters, justifying thus the use of *RCC*. To take into account the possible correlation between input parameters, the partial rank coefficients of correlation (*PRCC*) between an input pa-

rameter X_i and an output parameter Y was calculated as follows:

$$PRCC[Y, X_i] = -\frac{C_{iY}^{-1}}{\sqrt{C_{ii}^{-1} C_{YY}^{-1}}} \quad (8)$$

where C^{-1} is the inverse matrix of C:

$$C = \begin{bmatrix} 1 & r_{12} & \cdots & r_{1N} & r_{1Y} \\ r_{21} & 1 & \cdots & r_{2N} & r_{2Y} \\ \vdots & \vdots & \ddots & \vdots & \vdots \\ r_{N1} & r_{N2} & \cdots & 1 & r_{NY} \\ r_{Y1} & r_{Y2} & \cdots & r_{YN} & 1 \end{bmatrix} = \begin{bmatrix} A & B \\ B^T & 1 \end{bmatrix} \quad (9)$$

where A was the input parameters correlation matrix with elements $r_{ij} = RCC$ and B was the input-output correlation vector with elements r_{jY}. A positive PRCC value indicates that the output parameter increases with the input parameter, and vice versa.

To understand the relative determinant roles of input parameters on the effect of dose omission, the score (SC_i) was defined from the input-output PRCC value as follows:

$$SC_i = \frac{|PRCC(Y, X_i)|}{\sum_{i=1}^{m} |PRCC(Y, X_i)|} \quad (10)$$

where i = 1,2,...m.

Once the estimated PRCC values and scores were obtained using N=1000 simulated drugs, the results were used for the classification of n chosen drugs in terms of their forgiveness. The classification process can be direct if a single parameter emerges as the most sensitive one. However, it is possible that more than one parameter were identified as important, for which case a more delicate criterion, based on the scores, to delineate drugs forgiveness was developed.

2.7. Drug Forgiveness Estimation: Comparative Drug Forgiveness Index (CDFI)

The defined scores to compare n drugs in terms of their forgiveness were illustrated. For this, the concept of Comparative Drug Forgiveness Index (CDFI) was introduced and calculated for the n considered drugs from the class of calcium channel blockers.

For each drug, CDFI was directly computed from its PK and PD parameters and the predetermined scores of the corresponding pharmacological class. This made CDFI an accessible method easily applicable in practice for drug forgiveness classification.

2.8. Calculation of CDFI

Assume m PK/PD parameters were used for each of the n considered drugs; each parameter was represented by a vector $\mathbf{X}_i = (X_{i1}, X_{i2}, \cdots X_{in})$, i = 1, 2, …, m, with each component corresponding to the i-th PK/PD parameter of one drug. $\mathbf{Y}$ was the n-ry vector of the corresponding compliance index, namely SD and SI. SC_i is the score of $\mathbf{X}_i$ defined by Equation 10.

Depending on $PRCC(Y, \mathbf{X}_i)$ values and considering that an increase of a given compliance index positively or negatively influences the therapeutic outcome, the forgiveness index F_{ij} was defined to measure the relative performance of the i-th parameter X_{ij} of the j-th drug in terms of drug forgiveness.

To calculate F_{ij}, the drug index j_0 for which X_{ij_0} indicates, in terms of drug forgiveness, the worst performance among X_{ij}, j = 1, 2, …, n was first determined. The different cases are summarized as follows:

1) An increase in compliance index negatively influences the therapeutic outcome (e.g., an increase in *SD* negatively influences blood pressure control)

a) If $PRCC(Y, \mathbf{X}_i) > 0$, $j_0 = argmax_j(X_{ij})$ and we let $F_{ij_0} = -SC_i$

b) If $PRCC(Y, \mathbf{X}_i) < 0$, $j_0 = argmin_j(X_{ij})$ and we let $F_{ij_0} = SC_i$

2) An increase in compliance index positively influences the therapeutic outcome (e.g., an increase in *SI* positively influences blood pressure homogeneity)

a) If $PRCC(Y, \mathbf{X}_i) > 0$, $j_0 = argmin_j(X_{ij})$ and we let $F_{ij_0} = SC_i$

b) If $PRCC(Y, \mathbf{X}_i) < 0$, $j_0 = argmax_j(X_{ij})$ and we let $F_{ij_0} = -SC_i$

Hence the forgiveness index F_{ij} for the i-th parameter of the j-th drug was defined as follows:

$$F_{ij} = \begin{cases} F_{ij_0} & \text{if } j = j_0 \\ \dfrac{X_{ij} \times F_{ij_0}}{X_{ij_0}} & \text{if } j \neq j_0 \end{cases} \quad (11)$$

Table 2 illustrates a simplified diagram for the computation of the forgiveness index.

Table 2. A simplified diagram of the forgivness index calculation $\nearrow(\searrow)$ indicates an increase (decrease).

	$Y \nearrow \Rightarrow$ Terapeutic Outcome $\nearrow$	$Y \nearrow \Rightarrow$ Terapeutic Outcome $\nearrow$
$PRCC(\mathbf{Y}, \mathbf{X}_i) > 0$	$F_{ij} = X_{ij} \times SC_i / \min_j(X_{ij})$	$F_{ij} = X_{ij} \times (-SC_i) / \max_j(X_{ij})$
$PRCC(\mathbf{Y}, \mathbf{X}_i) < 0$	$F_{ij} = X_{ij} \times (-SC_i) / \max_j(X_{ij})$	$F_{ij} = X_{ij} \times SC_i / \min_j(X_{ij})$

3) For the *j*-th drug, $j = 1, 2, \ldots, n$, the Comparative Drug Forgiveness Index (CDFI) was defined by summing its individual forgiveness indices F_{ij}:

$$CDFI(j) = \sum_{i=1}^{m} F_{ij} \quad (12)$$

4) Finally, a ranking of drugs was based one their CDFI values, where a higher CDFI indicates a better drug forgiveness.

2.9. Application of CDFI

To evaluate the relevance and robustness of the approach defined here for the evaluation of drugs in terms of their forgiveness, CDFI for four long-action calcium channel blockers, namely benidipine, nivaldipine, manidipine and felodipine were calculated. Concentration and blood pressure data used in the study were obtained from literature [22,27,28] and were used for each of these drugs. The two compartment model generally adopted for these drugs in literature was used to estime the relevant PK and PD parameters using WinNonlin software package (Pharsight Corporation, Mountain View, CA, USA). The estimated values of PK and PD parameters were summarized in **Table 3**.

As observed in **Table 3**, large differences in PK and PD properties exist between the four calcium channel inhibitors investigated, assuring thus the robustness of the approach. Upon these disposition and effect models, the previously mentioned three compliance models were applied to these drugs to generate data for the assessment of their forgiveness.

3. Results

3.1. Exploratory Analysis of Input-Output Relationships

To check for the monotonicity in the input-output relationships, scatter plots representing the input parameters vs the model output SI were displayed in **Figure 3**. For each of the $m = 9$ input parameters $N = 1000$ copies were simulated.

Linear trends as well as nonlinear ones were displayed by these pairs. The monotonicity exhibited by these linear and nonlinear relationships justified our use of the rank coefficient of correlation (RCC) approach or the partial rank coefficient of correlation (PRCC). The latter was identified as the most appropriate and powerful method when parameters were correlated. In **Figures 4** and **5**, results of the RCC and PRCC of each input parameters with outcome parameters, SD and SI, when neglecting or not the correlations between various input parameters, respectively, are shown. Difference parameters rankings were obtained using these two approaches. For example, RCC identified K_e, K_{12}, K_{off} as the most important parameters for SD, whereas K_{off}, K_{on} and K_{21} were those identified by PRCC. The result rationalizes the choice for the PRCC approach in this study.

The PRCC values in **Figure 4** indicate that both output parameters, SD and SI, were sensitive to K_{off}, and at a less extent to K_{on} and K_{21}. The latter parameter belongs to the PK model while the two others to the PD model. While the ranking of these three parameters was preserved, the sign of correlation was reversed as ex-

Table 3. PK and PD parameters of the four long-action calcium channel inhibitors; Data from Shimada and al., Kirsten and al. [22,27,28].

Parameters	Benedipine	Nivaldipine	Manidipine	Felodipine
PK				
$K_a\,(h^{-1})$	1.33	0.67	0.63	0.51
$K_e\,(h^{-1})$	0.50	0.42	0.32	0.20
$K_{12}\,(h^{-1})$	1.07	0.11	0.20	0.27
$K_{21}\,(h^{-1})$	0.73	0.01	0.16	0.013
$V_1\,(L)$	1323.20	562.23	1449.90	465.20
$V_2\,(L)$	3045.70	6044.50	1833.10	9402.40
PD				
$E_{max}\,(mHg)$	23.40	36.92	17.63	29.62
$K_{on}\,(ng.h^{-1})$	1.26	0.143	0.32	0.54
$K_{off}\,(h^{-1})$	0.012	0.37	0.13	0.21

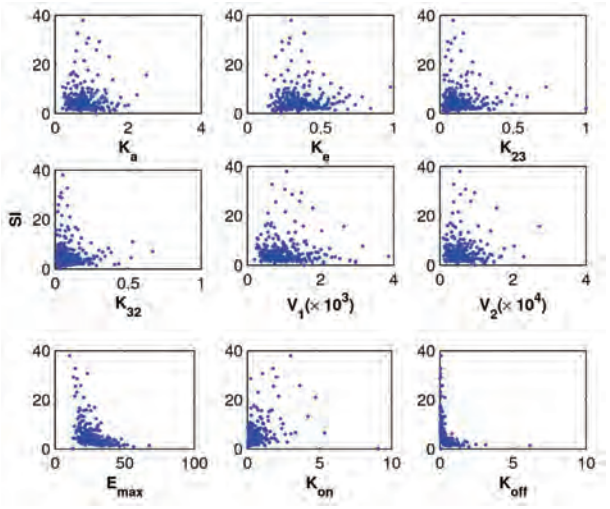

Figure 3. Correlation between PK and PD input parameters and SI.

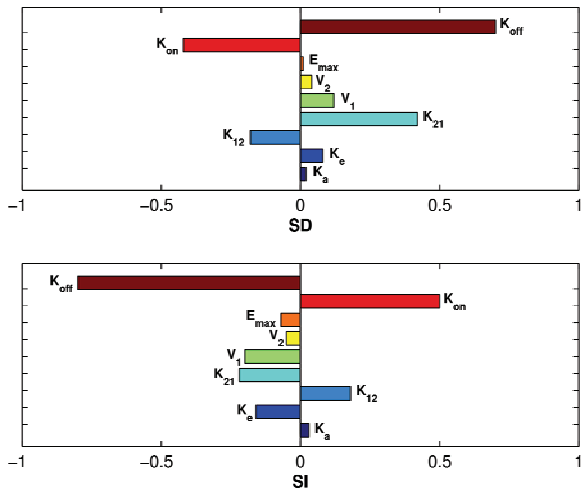

Figure 4. Coefficients of correlation between input and output parameters when possible input correlations are accounted for.

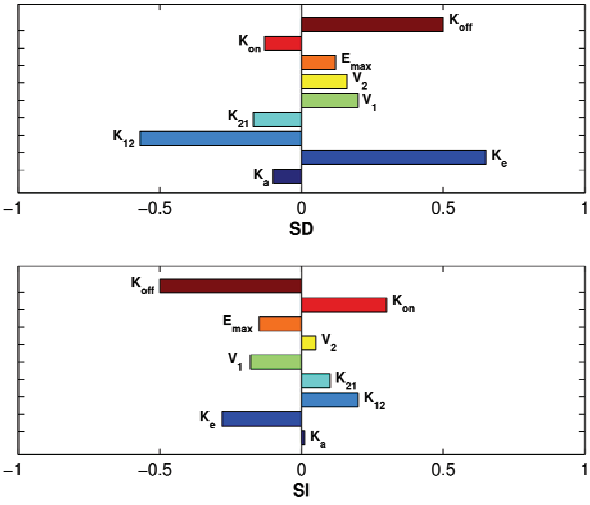

Figure 5. Coefficients of correlation between input and output parameters when input correlations are ignored.

pected as a consequence of the *SD* and *SI* definitions. From a clinical point of view, given two or more calcium channel blockers, this implied that drugs with smaller K_{off}, K_{21}, and larger K_{on} were preferred in terms of drug forgiveness. However, these conditions could be rarely satisfied for one drug at the same time, which led us to the development of a criterion for more general cases.

3.2. Choice of the Most Forgiving Drug Based on the Sensitivity of PK or PD Parameters

Three input parameters were identified as the most important ones, K_{on} and K_{off} were PD related while K_{21} was PK related. In terms of dose omission, nivaldipine was classified as the most forgiving drug if the delineation procedure is solely PK-based, while benedipine was the least forgiving one, as shown in **Table 3**. The conclusion may be reversed if the procedure was PD-based. Thus, a sensitivity analysis solely based on the PK properties while ignoring the PD component (and vice versa) could lead to erroneous classification of drugs. This result confirms the need to take into account as much PK/PD properties as possible for a proper characterization of drug tolerability to dose omissions.

3.3. Use of CDFI to Test Tolerability to Dose Omissions

The CDFI approach was applied in this study to classify the four calcium channel blockers in terms of their forgiveness to dose omissions. The PK/PD parameters of these four drugs (**Table 1**) were in the range of the Monte Carlo generated PK/PD parameters (**Table 1**), validating thus the use of PRCC method and consequently CDFI.

Since a sensitivity analysis was based only on PK or PD parameters, it cannot fulfill the task of classification, and therefore the CDFI approach was performed on these drugs as shown in **Table 4**.

For both output parameters, benidipine showed the highest CDFI, which means it holds for the longest effective therapeutic period and causes the least inhomogeneity in blood pressure. It was followed by manidipine for *SD* and by felodipine for *SI*.

3.4. CDFI Classification versus Direct Classification

Compared to direct classification approaches based on therapeutic markers, which require specific simulations for each drug, the advantage of CDFI was obvious. Moreover, CDFI was computed with the same compliance scenario to classify a whole pharmacological class, having a wide range of PK and PD properties. However, it was important to ensure the robustness of CDFI classification by considering different compliance patterns using direct classification approaches.

In this study, two therapeutic markers, namely *SD* or *SI*, can be used to study the performance of CDFI for the four chosen blockers by considering the three compliance scenarios above.

3.5. Compliance Scenario Using Markov Chain Model

In this study, 500 drug intake profiles were simulated for each drug using Markov chain approach to analyse the impact of drug intake irregularity on the therapeutic outcome. **Table 5** shows the values of several therapeutic markers that we calculated or extracted from the literature.

Table 4. Comparative drug forgiveness index for four long-action calcium channel drugs.

	Benedipine	Nivaldipine	Manidipine	Felodipine
CDFI(SD)	−10	−47	−27	−58
CDFI(SI)	51	−3.8	10	16

Table 5. Values of compliance markers obtained after simulation and experimental data.

Therapeutic marker	Benedipine	Nivaldipine	Manidipine	Felodipine
SD (h)	1.3	70.6	17.5	80.45
SI	8	0.13	0.59	1.13
Experimental SI	2[a]	-	0.6[b]	1[c]

[a]Data from Nakajima and al. [32]; [b]Data from Roca-Cusachs and al. [34]; [c]Data from Mancia and al. [31]

In terms of *SD*, benedipine, with the least therapeutic time of 1.3 *h*, had the best forgiveness. Manidipine was ranked second with *SD* = 17.5 *h*, while felodipine had the worst forgiveness with an SD of 80.45 h. When it comes to *SI*, benidipine and felodipine with SI value of 8 and 1.3 respectively, manifest their fine quality in the control of harmful fluctuations in blood pressure compared to the other two drugs. These results were consistent with those found using CDFI (**Table 4)**. Moreover, simulated *SI* was in accordance with experimental *SI* reported in literature from real data, which was a strong indication of the suitability of this study.

3.6. Noncompliance Based on Drug Holidays

Different scenarios based on the number of drug holidays, going from 1 to 15 times, each lasting exactly three days were explored. In this method, the perfect compliance was simulated into which a number of occasional drug holidays were used. **Figure 6** shows the relationship between *SD*, *i.e.*, number of subtherapeutic days, and number of drug holidays for different fixed systolic blood pressure deviations Δ*E*. With nivaldipine, the percentage of subtherapeutic days exceeds 10% after five drug holidays for Δ*E* = 0.2. However, when Δ*E* = 0.1, only benedipine showed an *SD* under 10%. It was noted that benedipine showed a better tolerance for drug holidays compared to the other drugs.

In **Figure 7**, the evolution of *SI* for each drug versus the number of drug holidays was shown. Benedipine had the largest *SI* decreasing ratio compared to other drugs. However, *SI* for nivaldipine and felodipine were almost not altered by drug holidays. This indicates that drug

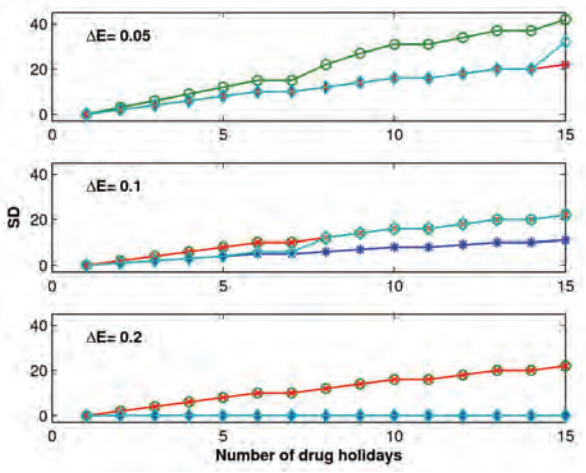

Figure 6. Number of days that a patient is inefficiently treated vs. number of drug holidays. ∗ = Benedipine; ◊ = Manidipine; × = Felodipine and ○ = Nivaldipine.

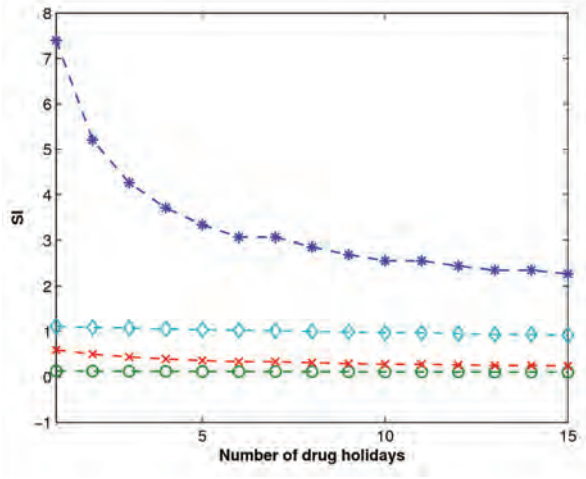

Figure 7. Profile of smoothness index vs. number of drug holidays. ∗ = Benedipine; ◊ = Manidipine; × = Felodipine and ○ = Nivaldipine.

omission had almost no influence on blood pressure fluctuation. Therefore, the difference between perfect and poor compliers in terms of organ damage induced by drug holidays can be neglected during hypertension treatment. These results were consistent with the CDFI classification (**Table 4**).

3.7. Noncompliance Based on Percentage of Taken Doses

For a fixed total dose, scenarios were simulated with an increasing percentage of taken doses, ranging from 10% to 100%. For each percentage of taken doses, percentage of subtherapeutic days (*SD*) was calculated; the results are shown in **Figure 8**. Similar to the compliance model

based on drug holidays, benedipine had a better forgiveness for dose omission, followed by manidipine. The other two drugs showed very poor forgiveness.

However, in terms of *SI*, benedipine changed more rapidly against percentage of taken doses than other drugs (**Figure 9**), which suggests a high risk of organ damages for non compliant patients during hypertension treatment. The above results were again consistent with the CDFI classification (**Table 4**).

4. Discussion

Many therapeutic strategies consider the issue of drug compliance as crucial for a treatment to be efficient. In this context, two options can be put forward under different philosophies, one is centered around the patient while the other targets the patient drug use. The first builds on the interactive synergy between the health caregiver and the patient, with the ultimate goal of the patient to be an integral part of drug execution. Since this approach heavily depends on the patient willingness and collaboration, it can be time consuming and provides no guarantee of improvement in patient drug intake. This has led to consider alternative drug-based strategies, with attempt to favor drugs that are more tolerable to the irregular drug intake, thus reducing the risk for therapeutic failure. This is particularly relevant for specific populations where compliance to medication has proved to be poor. The drug forgiveness issue has been raised by Urquhart [35], and suggested as an additive criterion in the drug evaluation. In the drug selection process, the characterization of PK/PD properties is crucial. Restricted by clinical and ethical conditions, a M&S approach can play a major role for this purpose. A step towards this direction has been made by Nony and coworkers [36].

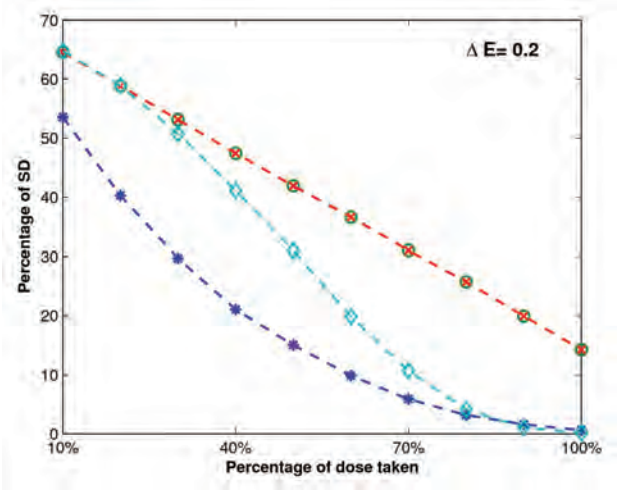

Figure 8. Number of days, the patient is inefficiently treated vs. percentage of taken doses. ∗ = Benedipine; ◊ = Manidipine; × = Felodipine and ○ = Nivaldipine.

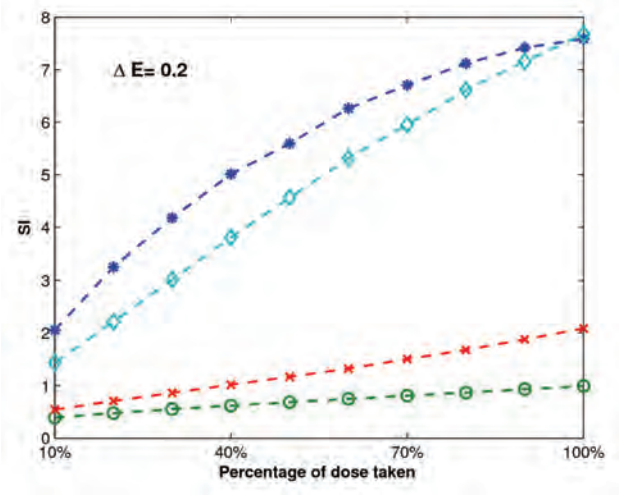

Figure 9. Profile of smoothness vs. percentage of dose taken. ∗ = Benedipine; ◊ = Manidipine; × = Felodipine and ○ = Nivaldipine.

In this study, a global sensitivity analysis (GSA) approach was adopted, that considers a whole package of PK/PD parameters and quantifies their roles on therapeutic outcomes in terms of compliance. For this, a previously developed GSA method was used and aimed at identifying important input parameters and quantify their influence on drug distribution in different tissues [15]. GSA incorporates the correlations between input parameters in the quantification of their influence on the model outcomes.

This approach for a PK and PD model was related to a compliance model. As a case-study, four calcium channel blockers with different PK/PD parameters have been tested. Using those PK and PD parameters identified as important by GSA, the drug classification in terms of forgiveness can be different whether the PK and/or PD models have been included or not. This indicates that considering the PK/PD parameters as independent variables can lead to erroneous conclusions. For instance, for drugs acting through direct effect model, the one having a very long elimination half-life is considered more forgiving. However, for drugs acting through indirect model, the one with the longest elimination half-life cannot be automatically judged as the most forgiving since the dissociation rate constant may also have an influence on the length of drug effect.

For the calcium channel blockers considered in this paper, the GSA approach reveals that the high degree of benedipine forgiveness is in part related to PD properties (K_{off} and K_{on}), while it can be more linked to PK properties (K_{21}) for the case of felodipine.

For the same pharmacology class drugs, it is difficult to classify drugs in terms of their forgiveness when several parameters simultaneously influence the drug response expressed through compliance indices. Our study raises the issue of the validation of those studies involving the sole knowledge of PK or PD components without consideration of the whole drug intake-PK/PD process. In this work, the GSA-based CDFI approach, which takes into account the unavoidable and complex relationship between these three components, can be used as a reasonable tool for the classification of drugs in terms of their forgiveness.

The results obtained in this study are reassuring and support the relevance of CDFI approach. Indeed, the drug forgiveness classification is consistent with the clinical results, which confirm the efficacy and long-action effect of the benedipine and manidipine compared to other calcium channel antagonists [37,23,34]. Moreover, simulated *SI* are also close to clinical data (see **Table 5**), indicating that benedipine induces high homogeneity of blood pressure, followed by felodipine and manidipine [30-34].

This work, which uses for the first time the global sensitivity analysis to compare drugs in terms of their forgiveness is a step forward towards a strategy that favor drugs that are more tolerable to deviations in drug executions.

5. Conclusions

In this work, a global sensitivity analysis has been performed to identify the most sensitive parameters to dose omissions. A Comparative Drug Forgiveness Index (CDFI), designed to rank drugs in terms of their tolerability to non compliance, has been proposed. The classification results are in accordance with what has been previously reported for the calcium channel blockers. The classification method developed here proved to be a powerful quantitative way to delineate drugs in terms of their forgiveness and provides a complementary decision rule for clinical and experimental studies.

6. Acknowledgements

This work has been supported by the NSERC and FRSQ grants held by Dr. Fahima Nekka. The Mathematical Centre of Excellence (MITACS) and Ivory Coast Republic are also acknowledged for their support.

REFERENCES

[1] B. Vrijens, G. Vincze, P. Kristanto, J. Urquhart and M. Burnier, "Adherence to Prescribed Antihypertensive Drug Treatments: Longitudinal Study of Electronically Compiled Dosing Histories," *British Medical Journal*, Vol. 336, No. 7653, 2008, pp. 1114-1117.

[2] J. Urquhart, "Patient Non-Compliance with Drug Regimens: Measurement, Clinical Correlates, Economic Impact," Eur Heart J., Vol. 17, No. (Suppl. A), 1996, pp. 8-15.

[3] R. Düsing, "Adverse Events, Compliance, and Changes in Therapy," *Current Hypertension Reports*, Vol. 3, No. 6, 2001, pp. 488-492.

[4] J. Urquhart, "Pharmacodynamics of Variable Patient Compliance: Implications for Pharmaceutical Value," *Advanced Drug Delivery Reviews*, Vol. 33, No. 3, 1998, pp. 207-219.

[5] P. Girard, L. B. Sheiner, H. Kastrissios and T. F. Blaschke, "Do we Need Full Compliance Data for Population Pharmacokinetic Analysis?" *J Pharmacokinetics and Biopharmaceutics*, Vol. 24, No. 3, 1996, pp. 265-282.

[6] A. Blesius, S. Chabaud, M. Cucherat, P. Mismetti, J. P. Boissel and P. Nony, "Compliance-Guided Therapy: A New Insight into the Potential Role of Clinical Pharmacologists," *Clinical Pharmacokinetics*, Vol. 45, No. 1, 2006, pp. 95-104.

[7] J. Li and F. Nekka, "A Probabilistic Approach for the Evaluation of Pharmacological Effect Induced by Patient Irregular Drug Intake," *Journal of Pharmacokinetics and Pharmacodynamics*, Vol. 36, No. 3, 2009, pp. 221-238.

[8] G. D. Gohore Bi, J. Li and F. Nekka, "Antimicrobial Breakpoint Estimation Accounting for Variability in Pharmacokinetics," *Theoretical Medicine and Biology*, Vol. 26, No. 6, 2009, p. 10.

[9] B. Vrijens, E. Goetghebeur, E. de Klerk, R. Rode, S. Mayer and J. Urquhart, "Modelling the Association between Adherence and Viral Load in HIV-Infected Patients," *Statistics in Medicine*, Vol. 24, No. 17, 2005, pp. 2719-2131.

[10] Y. Huang, S. L. Rosenkranz and H. Wu, "Modeling HIV Dynamics and Antiviral Response with Consideration of Time-Varying Drug Exposures, Adherence and Phenotypic Sensitivity," *Mathematical Biosciences*, Vol. 184, No. 2, 2003, pp. 165-186.

[11] E. Hénin, B. You, B. Tranchand, G. Freyer and P. Girard, "Issues of the Study of Patient Compliance to Treatment with Oral Anticancer Chemotherapy: Advantages of Pharmacokinetics-Pharmacodynamics Modelisation," *Therapie*, Vol. 62, No. 2, 2007, pp. 77-85.

[12] J. Li and F. Nekka, "A Pharmacokinetic Formalism Explicitly Integrating the Patient Drug Compliance," *Journal of Pharmacokinetics and Pharmacodynamics*, Vol. 34, No. 1, 2007, pp. 115-139.

[13] J. Li, C. E. Petit-Jetté, D. Gohore Bi, F. Fenneteau, R. J. Del Castillo and F. Nekka, "Assessing Pharmacokinetic Variability Directly Induced by Drug Intake Behaviour through Development of a Feeding Behaviour-Pharmacokinetic Model," *Journal of Theoretical Biology*, Vol. 251, No. 3, 2008, pp. 468-479.

[14] P. Nony and J. P. Boissel, "Use of Sensitivity Functions to Characterise and Compare the Forgiveness of Drugs,"

Clinical Pharmacokinetics, Vol. 41, No. 5, 2002, pp. 371-380.

[15] F. Fenneteau, J. Li and F. Nekka, "Assessing Drug Distribution in Tissues Expressing P-Glycoprotein Using Physiologically Based Pharmacokinetic Modeling: Identification of Important Model Parameters through Global Sensitivity Analysis," *Journal of Pharmacokinetics and Pharmacodynamics*, Vol. 36, No. 6, 2009, pp. 495-522.

[16] F. Fenneteau, P. Poulin and F. Nekka, "Physiologically Based Predictions of the Impact of Inhibition of Intestinal and Hepatic Metabolism on Human Pharmacokinetics of CYP3A Substrates," *Journal of Pharmaceutical Sciences*, Vol. 99, No. 1, 2010, pp. 486-514.

[17] A. Saltelli, S. Tarantola, F. Campolongo and M. Ratto, "Sensitivity Analysis in Practice: A Guide to Assessing Scientific Model," Wiley, New York, 2004.

[18] A. Saltelli, M. Ratto, S. Tarantola and F. Campolongo, "Sensitivity Analysis for Chemical Models," *Chemical Reviews*, Vol. 105, No. 7, 2005, pp. 2811-2828.

[19] J. Zàdor, I. G. Zsély, T. Turanyi, M. Ratto, S. Tarantola and A. Saltelli, "Local and Global Uncertainty Analyses of a Methane Flame Model," *Journal of Physical Chemistry A*, Vol. 109, No. 43, 2005, pp. 9795-9807.

[20] P. Girard, T. F. Blaschke, H. Kastrissios, L. B. Sheiner, "A Markov Mixed Effect Regression Model for Drug Compliance," *Statistics in Medicine*, Vol. 17, No. 20, 1998, pp. 2313-2333.

[21] J. Sun, H. N. Nagaraj, N. R. Reynolds, "Discrete Stochastic Models for Compliance Analysis Based on an AIDS Clinical Trial Group (ACTG) Study," *Biomedicine Journal*, 2007, Vol. 49, No. 5, pp. 731-741.

[22] S. Shimada, Y. Nakajima, K. Yamamoto, Y. Sawada and T. Iga, "Comparative Pharmacodynamics of Eight Calcium Channel Blocking Agents in Japanese Essential Hypertensive Patients," *Biological and Pharmaceutical Bulletin*, Vol. 19, No. 3, 1996, pp. 430-437.

[23] K. Yao, K. Nagashima and H. Miki, "Pharmacological, Pharmacokinetic, and Clinical Properties of Benidipine Hydrochloride, a Novel, Long-Acting Calcium Channel Blocker," *Journal of Pharmacological Sciences*, Vol. 100, No. 4, 2006, pp. 243-261.

[24] H. Y. Yun, M. H. Yun, W. Kang and K. I. Kwon, "Pharmacokinetics and Pharmacodynamics of Benidipine Using a Slow Receptor-Binding Model," *Journal of Clinical Pharmacy and Therapeutics*, Vol. 30, No. 6, 2005, pp. 541-547.

[25] R. B. Haynes, D. L. Sackett, E. Gibson, H. Wand, R. S. Roberts, *et al.*, "Improvement of Medication Compliance in Uncontrolled Hypertension," *Lancet*, Vol. 1, No. 7972, 1976, pp. 1265-1268.

[26] A. Saltelli, M. Ratto, T. Andres, F. Campolongo, J. Cariboni, D. Gatelli, *et al.*, "Global Sensitivity Analysis: The Primer," Wiley, Chichester, 2008.

[27] Y. Nakajima, K. Yamamoto, S. Shimada, H. Kotaki, Y. Sawada and T. Iga, "In Vitro-in Vivo Correlation of Pharmacodynamics of Felodipine in Essential Hypertensive Patients Based on an Ion-Channel Binding Model," *Biological and Pharmaceutical Bulletin*, Vol. 19, No. 8, 1996, pp. 1097-1099.

[28] R. Kirsten, K. Nelson, D. Kirsten and B. Heintz, "Clinical Pharmacokinetics of Vasodilators," *Part I. Clinical pharmacokinetics*, Vol. 34, No. 6, 1998, pp. 457-482.

[29] O. Nakajima, H. Akioka and M. Miyazaki, "Effect of the Calcium Antagonist Benidipine Hydrochloride on 24-h Ambulatory Blood Pressure in Patients with Mild to Moderate Hypertension in a Double-Blind Study against Placebo," *Arzneimittelforschung*, Vol. 50, No. 7, 2000, pp. 620-625.

[30] G. Mancia, S. Omboni, E. Agabiti-Rosei, R. Casati, R. Fogari, G. Leonetti, *et al.*, "Antihypertensive Efficacy of Manidipine and Enalapril in Hypertensive Diabetic Patients," *Journal of Cardiovascular Pharmacology*, Vol. 35, No. 6, 2000, pp. 926-931.

[31] S. R. O. Antonicelli, D. C. Giovanni, R. Ansuini, A. Mori, R. Gesuita, G. Parati, *et al.*, "Smooth Blood Pressure Control Obtained with Extended-Release Felodipine in Elderly Patients with Hypertension: Evaluation by 24-Hour Ambulatory Blood Pressure Monitoring," *Drugs Aging*, Vol. 19, No. 7, 2002, pp. 541-551.

[32] G. Mancia, S. Omboni, G. Parati, D. L. Clement, W. E. Haley, S. N. Rahman, *et al.*, "Twenty-Four Hour Ambulatory Blood Pressure in the Hypertension Optimal Treatment (HOT) Study," *Journal of Hypertension*, Vol. 19, No. 10, 2001, pp. 1755-1763.

[33] S. Omboni, R. Fogari and G. Mancia, "A Smooth Blood Pressure Control is Obtained over 24 h by Delapril in Mild to Moderate Essential Hypertensives," *Blood Press*, Vol. 10, No. 3, 2001, pp. 170-175.

[34] A. Roca-Cusachs and F. Triposkiadis, "Antihypertensive Effect of Manidipine," *Drugs*, Vol. 65, No. (Suppl. 2), 2005, pp. 11-19.

[35] J. Urquhart, "Erratic Patient Compliance with Prescribed Drug Regimens: Target for Drug Delivery Systems," *Clinical Pharmacology & Therapeutics*, Vol. 67, No. 4, 2000, pp. 331-334.

[36] J. P. Boissel and P. Nony, "Using Pharmacokinetic-Pharmacodynamic Relationships to Predict the Effect of Poor Compliance," *Clinical Pharmacokinetics*, Vol. 41, No. 1, 2002, pp. 1-6.

[37] S. M. Cheer and K. McClellan, "Manidipine: A Review of its Use in Hypertension," *Drugs*, Vol. 61, No. 12, 2001, pp. 1777-1799.

Pharmacology & Pharmacy, **2010, 1, 53-59**
doi:10.4236/pp.2010.12008 Published Online October 2010 (http://www.SciRP.org/journal/pp)

Antioxidant Effect of Atorvastatin in Type 2 Diabetic Patients

Najah R. Hadi[1], Mohammad A. Abdelhussein[2], Omran M. O. Alhamami[1], Ammar R. Muhammad Rudha[1], Ekhlas Sabah

[1]Department of Pharmacology, Faculty of Medicine, Kufa University, Najaf, Iraq; [2]Department of Medicine, Faculty of Medicine, Kufa University, Najaf, Iraq.
Email: drnajahhadi@yahoo.com

Received August 26th, 2010; revised September 12th, 2010; accepted September 20th, 2010.

ABSTRACT

Evidence has long been existed regarding the relationship between oxidative stress and diabetes. The present study was conducted to assess the effect of atorvastatin on selected oxidative stress parameters and its effect on lipid profile parameters in dyslipidaemic type 2 *diabetic patients. Fifty nine dyslipidaemic type* 2 *diabetic patients were included in this study. A full history was taken and general examination was performed. The patients were taking an oral hypoglycaemic drug* (*glibenclamide*) *during the study. The patients were followed up for* 60 *days and divided randomly into* 2 *groups. Group I* (*n* = 31) *received no drug and served as dyslipidaemic diabetic control. Group II* (n = 28) *received atorvastatin tablets* 20 *mg once daily at night. Blood samples were drawn from the patients at the beginning and after* 60 *days of follow up between* 8:30 *and* 10:30 *am after at least* 12-14 *hours fasting. Fasting blood glucose, lipid profile, selective oxidative stress parameters, glutathione S reductase* (*GSH*), *malondialdehyde* (*MDA*) *levels, glutathione S transferase* (*GST*) *and catalase* (*CAT*) *activities were measured. Renal and hepatic functions were also assessed. The results showed that atorvastatin treatment produced significant increase in serum levels of GSH and High Density Lipoprotein* (*HDL*), *while serum levels of MDA, Total Cholesterol* (*TC*), *Triglyceride* (*TG*), *Low Density Lipoprotein Cholesterol* (*LDL-C*) *and Very Low Density Lipoprotein* (*VLDL*) *were significantly decreased. However, no significant effect was observed regarding CAT and GST activity. There were insignificant correlations between atorvastatin induced changes in the oxidation markers and the observed changes of the lipid profile. In conclusion, the antioxidant effect of atorvastatin could be unrelated to its hypolipidemic action as there was insignificant correlation between changes in lipid profile and oxidative stress in this study.*

Keywords*: *Atorvastatin, Type* 2 *Diabetes, Oxidative Stress, Dyslipidaemia

1. Introduction

Oxidative stress is defined as tissue injury resulting from a disturbance in the equilibrium between the production of reactive oxygen species (ROS) (also known as free radicals) and antioxidant defense mechanisms [1]. Under physiologic conditions, the antioxidant defenses are able to protect against the deleterious effects of ROS, but under conditions where either an increase in oxidant generation, a decrease in antioxidant protection or a failure to repair oxidative damage, accumulation of free radicals ensures, leading to cellular and tissue damage [2]. Excess generation of ROS in oxidative stress have pathological consequences including damage to polyunsaturated fatty acids in membrane lipids, proteins, DNA and ultimately cell death [3]. ROS have been implicated in many disease state including neurodegenerative disease like

Alzheimer's and Parkinson's disease, atherosclerosis, inflammatory conditions, certain cancers, diabetes mellitus (DM), cataract in the eye, pulmonary, renal, heart diseases and the process of aging [4,5]. Diabetes mellitus is a group of metabolic disorders with one common manifestation: hyperglycaemia associated with defects in insulin secretion, action or both. Traditionally it has been classified into two forms Type 1 DM and Type 2 DM [6]. Type 2 DM which is known to be multifactorial, resulting from combination of various factors such as impaired fatty acid metabolism, central fat deposition leading to insulin resistance in various tissues (liver, muscles, adipose) [7], beta-cell secretary defect and obesity [4]. Evi-

dence has long existed regarding the relationship between oxidative stress and DM [8]. Eisei N. *et al.* postulated that oxidative stress is involved in the onset and progression of diabetes, initiation and exacerbation of micro- and macrovascular complications in diabetes and recently oxidative stress status markers have been associated directly with the severity and prognosis of diabetes [9]. There are multiple sources of oxidative stress in DM, including non enzymatic (glucose autoxidation, non enzymatic glycation of proteins), enzymatic (NADPH oxidase, nitric oxide synthase) and mitochondrial pathway [10].

Dyslpidaemia is used to describe a group of conditions in which there are abnormal levels of lipid and lipoprotein in the blood [11]. In type 2 diabetes, dyslipidaemia is characterized by elevated circulating levels of TG, decreased circulating levels of HDL and usually accompanied by an elevation of small dense LDL-cholesterol particles [12]. There is an evidence indicating that hyperlipidaemia is associated with enhanced oxidative stress [13]. Atorvastatin belongs to 3-hydroxy-3-methylglutaryl-coenzyme A (HMG-CoA) reductase inhibitors, (or statins) which are potent inhibitors of cholesterol biosynthesis that are used extensively to treat patients with hypercholesterolaemia [14,15]. Atorvastatin is a synthetic lipid lowering agent [16]. It is a competitive inhibitor of HMG-CoA reductase which catalyzes the conversion of HMG-CoA to mevalonate, an early rate limiting step in cholesterol biosynthesis resulting in depletion the intracellular supply of cholesterol [17]. Inhibition of cholesterol biosynthesis is accompanied by an increase in hepatic LDL receptor on the cell surface which promotes uptake and clearance of circulating LDL. Thus the end result is a reduction in plasma cholesterol by both lowered cholesterol synthesis and by increased catabolism of LDL [15]. Atorvastatin also reduces VLDL-C, TG and produces variable increase in HDL-C [18]. Atorvastatin is safe and generally well tolerated [19]. Mild gastrointestinal side effects like dyspepsia, flatulence, abdominal pain, diarrhea and constipation may occur. Other side effects include headache, rash, pruritus and malaise. The most detrimental adverse effect of atorvastatin is hepatotoxicity and myopathy [20].

Munford [21] and Shishehbor *et al.* [22] stated that the overall clinical benefits observed with atorvastatin therapy appear to be greater than what might be expected from changes in lipid levels alone, suggesting effects beyond cholesterol lowering called pleiotropic effects. Vishal *et al.* indicated that some of the cholesterol-independent effects of atorvastatin involve improving endothelial function, enhancing the stability of atherosclerotic plaques, decreasing oxidative stress, decreasing inflammation, improve insulin resistance, inhibiting the thrombogenic response in the vascular wall and impede tumor cells. Further more statin have other extrahepatic beneficial effects on the immune system, central nervous system and bone [23]. Atorvastatin possesses antioxidant properties by reducing lipid peroxidation and ROS production [23]. It reduces the susceptibility of lipoproteins to oxidation both in vitro and in vivo, *i.e.*, they decrease the LDL oxidation [23].

The Aim of This Study was to clarify the effect of atorvastatin on selected oxidative stress parameters namely (reduced glutathione (GSH), lipid peroxidation product malondialdehyde (MDA) levels, glutathione –S-transferase (GST) and catalase (CAT) activities) and lipid profile in dyslipidaemic type 2 diabetic patients.

2. Materials and Methods

2.1. Materials

Atorvastatin (Atorfit 20, Ajanta Pharma Limited, India,), EDTA & GSH (Biochemicals Co. Ltd.), DTNB (Sigma Co. Ltd.), Trichloroacetic acid (TCA) & Thiobuteric acid (TBA) (Merk Co. Ltd.) were obtained as a gift samples. CDNB, K_2HPO_4, KH_2PO_4, Na_2HPO_4, H_2O_2 (Analar company) were purchased commercially and used as received.

2.2. Patients

Fifty nine patients (age: 57.16 ± 1.34 years; 32 men & 27 women) with type 2 DM and dyslipidaemia were included in this study after obtaining their written consent and formal approval of the human experimentation committee at the Faculty of Medicine, Kufa University. The mean fasting blood glucose was (7.91 ± 0.7 mmol/l), with a mean duration of diabetes of (8.4 ± 1.08 years). The mean LDL-C level was (5.48 ± 0.72 mmol/l). The patients were chosen randomly from Al- Hakeem center for researches and treatment of DM at Al-Sadr Teaching Hospital in Najaf City in the period between 5th Nov. 2006 to 24th June 2007. These patients underwent full history and complete physical examination. Patients with the following criteria were excluded from the study: 1) Patients who use any vitamin preparations, or statins in the last three months [24]; 2) Patients with renal insufficiency, defined as a serum creatinine level equal to or more than 1.8 mg/dl [24]; 3) Patients with liver disease [22]; 4) Hypertensive patients, as this condition affects oxidative stress [13] and antihypertensive drugs may affect lipid profile and oxidative stress in hypertensive patients [25,26]; 5) Patients with chronic inflammatory diseases [24]; 6) Alcoholics & smokers were also excluded [27]. The patients were using glibenclamide (Glibesyn, Medochemie LTD-Cyprus; Glibils, Hikma-Jordon) (an oral hypoglycaemic agent) during the study

as a treatment for their diabetes. According to the design of the study, type 2 diabetic patients were followed up for 60 days and divided randomly into two groups: Group I (n = 31) received no drug and served as dyslipidaemic diabetic control. Group II (n = 28): received atorvastatin tablets 20 mg once daily at night (Atorfit 20). Only forty six patients continued to the end of the study while thirteen patients were withdrawn (eight patients from Group I and five patients from Group II) because of non compliance. The patients were put on diet control and followed up every two weeks during the time of the study in order to make sure that they were using the medication properly and to regularly checking fasting blood glucose. Values of fasting blood glucose before, during and after the study were controlled within the previously mentioned range. Blood samples were drawn from the patients at the beginning and after 60 days of follow up between 8:30 & 10:30 am after at least 12-14 hours fasting. Fasting blood glucose, lipid profile, selected oxidative stress parameters (GSH, MDA levels, GST, CAT activities) were measured. Renal and hepatic functions were also assessed.

2.3. Sample Preparation

From each patient, 3 ml of blood was obtained without using heparin after an overnight fasting. The blood was placed in serum tube and left to stand for 30 minutes. The serum was prepared by centrifugation at 3000 rpm for 10 minute, 1.5 ml of serum was obtained for determination of experimental parameters which included GSH, MDA (the byproduct of lipid peroxidation), GST enzyme, CAT enzyme and lipid profile.

2.4. Serum Reduced Glutathione (GSH) Assay

Serum GSH was estimated according to a modified method of Ellman [28]. Briefly, Stock standard solution was prepared fresh daily by dissolving 0.0307 gm of GSH in a final volume of 100 ml of (0.2M) EDTA solution. Dilutions were made in EDTA solution to 50, 100, 150, 200, 250, 300, 400, 500 µM. The absorbance of this series of known concentrations was determined spectrophotometricaly using Shimadzu UV-1650P (UV-visible) at 412 nm to construct the calibration curve, "**Figure 1**".

2.5. Serum Lipid Peroxidation Product (MDA) Assay

The level of serum MDA was determined by a modified procedure described by Guidet and Shah [29]. Add 1 ml of TCA 17.5% and 1 ml of 0.6% thiobarbituric acid (TBA) to 0.15 ml of serum sample. The solution was mixed well by vortex, incubated in boiling water bath for 15 minutes, then allowed to cool. 1 ml of 70% TCA was

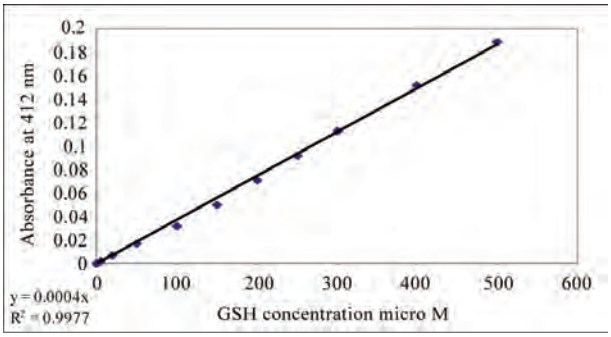

Figure 1. Standard curve for determination of reduced glutathione level.

added, and the mixture was allowed to stand at room temperature for 20 minutes, centrifuged at 2000 rpm for 15 minutes, and the supernatant was taken out for scanning spectrophotometrically at 532 nm using Shimadzu UV-1650P (UV-visible) Spectrophotometer.

$$\textit{The concentration of } MDA = \frac{\text{Absorbance } at\ 532\ nm}{\text{L} \times \epsilon} \quad (1)$$

L: Light path (1 cm)

ϵ: Extinction coeffoent $1.56 \times 105\text{M} \left|1.\text{Cm}\right| 1$

$$D : dilution\ factor = \frac{\text{Total volume}}{\text{Volume of the sample}}$$

2.6. Serum GST Enzyme Activity Assay

The absorption technique [30] includes mixing of 2.7 ml of Phosphate buffer (pH = 6.25) with 100 µL of serum and 100 µL of CDNB (1-chloro, 2, 4-dinitro benzene) and then after 3 minutes with 100 µL of GSH solution. After mixing the solutions, the absorbance was read every minute for 10 minutes at wave length 340 nm.

Calculation:

$$\textit{Activity of } GST \left(\frac{U}{L}\right) = \frac{\frac{\Delta A}{10} \times \text{Vt} \times 1000}{\epsilon \times \text{Vs} \times \text{b}} \quad (2)$$

ΔA = absorbance difference between the first and tenth minute

Vt = The total volume

Vs = Sample volume

ϵ = 9.6 mM-1cm-1

b = 1 cm.

$$\textit{Activity of } GST = \frac{\frac{\Delta A}{10} \times 3 \times 1000}{9.6 \times 0.1 \times 1} \quad (3)$$

2.7. Serum Catalase Activity Assay

The absorption technique [31] include mixing of 2 ml of

diluted serum with 1ml of H_2O_2 The solution was mixed well and the first absorbance (A1) was read after 15 seconds (t1) then the second absorbance (A2) after 30 seconds (t2) at a wave length 240 nm. 1 ml of Phosphate buffer solution was used instead of H_2O_2 for the blank solution.

Calculation:

$$K = \frac{Vt}{Vs} x2.\frac{3}{\Delta t} x log \frac{A1}{A2} x60 \quad (4)$$

K = rate constant of the reaction
Δt = (t2 – t1) 15 seconds
A1 = absorbance after 15 seconds
A2 = absorbanse after 30 seconds
Vt = total volume (3ml)
Vs = volume of the sample

2.8. Serum Lipid Profile Assay

Total cholesterol, Triglyceride and HDL were measured according to procedures supplied by Spinreact company kits, using Shimadzu UV-1650P (UV-visible)) Spectrophotometer. Serum LDL measure according to the following equation [32]

$$LDL = \text{total cholesterol} - HDL - VLDL \quad (5)$$

$$VLDL = TG/2.2. \quad (6)$$

2.9. Statistical Methods

The data expressed as mean ± SEM unless otherwise stated. Statistical analyses were done by using paired t-test. Pearson's correlations were also performed with significant difference set at $P < 0.05$.

3. Results

3.1. Effect of Atorvastatin on Oxidative Parameters

Atorvastatin treatment increased serum GSH and reduced MDA level significantly (P 0.05) while no significant change in serum GST and CAT activity was observed (P 0.05). There was no significant change (P 0.05) in oxidative stress parameters in diabetic control group apart from significant increase in MDA level "**Table 1**".

3.2. Effect of Atorvastatin on Lipid Profile

A significant decrease in serum TC, TG, LDL and VLDL and significant increase in HDL levels after atorvastatin treatment (P 0.05) while no significant change in lipid profile in diabetic control group was observed "**Table 2**".

3.3. Correlations between Observed Changes in Oxidation Markers and Observed Changes in Lipid Parameters in Atorvastatin Group

There were no significant correlations between atorvastatin induced changes in the oxidation markers and the observed changes in the lipid profile (P 0.05) "**Table 3**".

4. Discussion

4.1. Effect of Oxidative Stress Parameters

The significant increase in GSH and significant decrease in MDA levels (P 0.05) following atorvastatin treatment is supported by the findings of Save *et al.* [33] and Koter *et al.* [34], respectively. The most likely explanation for the increment of GSH and reduction of MDA by atorvastatin was attributed to the antioxidant mediated effect of atorvastatin which results from inhibition of mevalonate pathway. This effect results in a reduction in the synthesis of important intermediates including isoprenoids ((farnesyl pyrophosphate & geranylgeranyl pyrophosphate). The latter serve as lipid attachments for intracellular signaling molecules in particular inhibition of small GTPase binding proteins (Rho, Rac, Ras and G proteins) whose proper membrane localization and function are dependent on isoprenylation. These proteins modulate a variety of cellular processes including signaling, differentiation and proliferation [35,36]. Atorvastatin attenuates endothelial reactive oxygen species (ROS)

Table 1. Effect of atorvastatin (20 mg/day) on oxidative stress parameters after 60 days of treatment and changes in dyslipidaemic diabetic control (n = 23 in each group).

Parameters	Diabetic control		Atorvastatin	
	Before treatment	After treatment	Before treatment	After treatment
GSH(mmol/l)	0.24 ± 0.0079	0.22 ± 0.0036*	0.23±0.0034	0.40±0.0009**
MDA(mol/l)	1.25×10^{-4} ± 0.0146	1.59×10^{-4} ±0.0210**	1.24×10^{-4} ±0.0178	0.24×10^{-4} ± 0.004**
GST(U/l)	13.68 ± 0.18	13.87 ± 0.2194*	13.95 ± 0.234	14.07 ± 0.212*
CAT(K/ml)	0.49 ± 0.0123	0.5001 ± 0.016*	0.48 ± 0.0133	0.483 ± 0.012*

*p > 0.05; **p < 0.01; Values expressed as mean ± SEM.

Table 2. Effect of atorvastatin (20 mg/day) on lipid profile after 60 days of treatment and changes in dyslipidaemic diabetic control (n = 23 in each group).

Parameters	Diabetic control		Atorvastatin	
	Before treatment	After treatment	Before treatment	After treatment
TC(mmol/l)	6.99 ± 0.1173	6.74 ± 0.0332*	7.49 ± 0.0230	4.38 ± 0.0189**
TG(mmol/l)	2.78 ± 0.0645	2.68 ± 0.0159*	2.84 ± 0.0145	1.78 ± 0.0069**
HDL(mmol/l)	0.81 ± 0.0300	0.76 ± 0.0114*	0.76 ± 0.0159	1.06 ± 0.0109**
LDL(mmol/l)	4.90 ± 0.1300	4.75 ± 0.0339*	5.43±0.0243	2.51 ± 0.0168**
VLDL(mmol/l)	1.26 ± 0.0129	1.21 ± 0.0031*	1.29±0.0029	0.81 ± 0.0013**

*p > 0.05; **p < 0.01; Values expressed as mean ± SEM.

Table 3. Pearson's correlation for changes in the oxidative markers and lipid parameters in the atorvastatin group.

parameter	GSH	MDA	GST	CAT
TC	−0.232	0.042	0.427	−0.119
TG	−0.172	−0.105	0.039	−0.135
HDL-C	−0.223	−0.068	0.220	−0.139
LDL-C	−0.083	0.088	0.329	−0.032
VLDL-C	−0.157	0.001	−0.031	−0.055

P > 0.05 non significant.

formation, through attenuating endothelial superoxide anion production, by inhibition of NAD(P)H oxidase activity via Rho dependent mechanism. Some of antioxidant effects of atorvastatin may be due to its metabolites such as hydroxyl metabolites which have direct antioxidant effect. Atorvastatin improves and preserves the level of vitamin C, E and endogenous antioxidant such as reduced glutathione [16]. The protective effects of atorvastatin on ROS including cholesterol dependent and non cholesterol dependent antioxidative properties [16].

Serum GST enzyme activity did not significantly change in atorvastatin treatment and this finding was consistent with Passi *et al*. [37] who concluded that atorvastatin had no effect on GST activity.

It was also noted that atorvastatin showed insignificant change in the CAT activity which is in agreement with Passi *et al.* [37]. However, our results conflict with the findings of Wassmann *et al.* who concluded that atorvastatin caused a significant increase in the CAT activity [38]. This confliction may be due to the fact that the sample size may be relatively small permitting chance observations to exert substantial effects.

4.2. Effect on Lipid Profile

A significant decrease in serum level of TC, TG, LDL and VLDL and significant increase in serum level of HDL by atorvastatin treatment are in agreement with the findings obtained by Diabetes Atorvastatin Lipid Intervention study group [39] and Save *et al.* [33]. The mechanism involved is most likely attributed to the ability of atorvastatin to impair cholesterol synthesis via inhibiting the enzyme HMG-CoA reductase, which is the rate limiting step in cholesterol biosynthesis. This leads to both, decrease circulating lipoproteins and increase their uptake by up regulating hepatic LDL-C receptors. The overall lipid lowering effect include increase uptake and degradation of LDL-C, inhibition of LDL-C oxidation, reduction in cholesterol accumulation and esterification and decreases lipoprotein secretion and cholesterol synthesis [22,40].

4.3. Correlations between the Observed Changes in the Oxidation Markers and the Improvement of Lipid Profile in Atorvastatin

According to this study there were insignificant correlations between the observed changes in the pleiotropic effect of atorvastatin, regarding antioxidant properties and the improvement in the lipid profile. The same findings was reported by Sakabe *et al.* [41]. This pleiotropic effect of atorvastatin is due, predominantly, to inhibition of isopreniods but not cholesterol synthesis [42].

From the results of this study, we can conclude that, atorvastatin increased GSH, reduced MDA levels and had no effect on CAT and GST activities. Atorvastatin reduced TC, TG, LDL-C, VLDL-C and increased HDL-C levels. Also there were no correlations between the observed changes in the oxidation markers and the improvement of the lipid profile in the atorvastatin.

5. Conclusions

The antioxidant effect of atorvastatin could be unrelated to its hypolipidemic action as there was insignificant

correlation between changes in lipid profile and oxidative stress in this study.

6. Acknowledgements

Special thanks to everybody that help us in accomplishing this work.

REFERENCES

[1] D. J. Betteridge, "What is Oxidative Stress?" *Metabolism*, Vol. 49, No.2, 2000, pp. 3-8.

[2] B. Halliwell, "Free radicals, Antioxidants & Human Disease: Curiosity, Cause or Consequence," *Lancet*, Vol. 344, No. 8924, 1994, pp. 721-724.

[3] K. Kannan and S. K. Jain, "Oxidative Stress & Apoptosis," *Pathophysiology*, Vol. 7, No. 3, 2000, pp. 153-163.

[4] S. Shah, M. Iqbal, J. Karam, M. Salifu and S. I. Mcfarlane, "Oxidative stress, Glucose Metabolism & the Prevention of Ttype 2 Diabetes: Pathophyiological Insights," *Antioxidants & Rredox Signaling*, Vol. 9, No. 7, 2007, pp. 911-929.

[5] I. S. Young and J. V. Woodside, "Antioxidants in Health & Disease," *Journal of Clinical Pathology*, Vol. 54, No. 3, 2001, pp. 176-186.

[6] J. A. Florence and B. F Yeager, "Treatment of Type 2 Diabetes Mellitus," *American Family Physician*, Vol. 59, 1999, p. 10.

[7] J. L. Mehta, N. Rasouli, A. K. Sinha and B. Molavi, "Oxidative Stress in Diabetes: A mechanistic Overview of its Effects on Atherogenesis and Myocardial Dysfunction," *The International Journal of Biochemistry & Cell Biology*, Vol. 38, No. 5-6, June 2006, pp. 794-803.

[8] L. W. Oberley, "Free Radicals and Diabetes," *Free Radical Biology & Medicine*, Vol. 5, No. 2, 1988, pp. 113-124.

[9] N. Eisei and T. Hirokazu, "Parameters for Measurement of Oxidative Stress in Diabetes Mellitus: Applicability of ELISA for Clinical Evaluation," *Jòurnal of Investigation Medicine*, Vol. 53, No.4, May 2005, pp. 167-175.

[10] J. S. Johansen, A. K. Harris, D. J. Rychly and A. Ergul, "Oxidative Stress & the Use of Antioxidants in Diabetes: Linking Basic Science to Clinical Practice," *Cardiovascular Diabetology*, Vol. 4, April 2005, p. 5.

[11] J. Patel, "Dyslipidaemia in Diabetes," *British Midical Journal Clinical Evidence*, Vol. 8, No. 4, 2006, pp. 355-364.

[12] C. M. Florkowski, "Management of Co-Existing Diabetes Mellitus & Dyslipidaemia: Defining the Role of Thiazolidinediones," *American Journal of Cardiovascular Drugs*, Vol. 2, No. 1, 2002, pp. 15-21.

[13] F. Violi, L. Loffredo, L. Musella and A. Marcoccia, "Should Antioxidant Status be Considered in Interventional Trials with Antioxidants?" *Heart*, Vol. 90, No. 6, 2004, pp. 598-602.

[14] M. C. Sheffield, "Multiple Effects of Statins in Non Lipid Disease States," *US Pharmacist*, Vol. 6, 2004, pp. 38-54.

[15] J. K. Liao, "Isoprenoids as Mediators of the Biological Effects of Statins," *Journal Clinical Investigation*, Vol. 110, No. 3, August 2002, pp. 285-288.

[16] F. R. Danesh and Y. S. Kanwar, "Modulatory Effects of HMG-CoA Reductase Inhibitors in Diabetic Microangiopathy," *The FASEB Journal*, Vol. 18, No. 7, 2004, pp. 805-815.

[17] J. Beltowski, "Statins & Modulation of Oxidative Stress," *Toxicology Mechanisms & Methods*, Vol. 15, No. 2, 2005, pp. 61-92.

[18] B. B. Hodgson and R. J. Kizior, "Saunders Nursing Drug Handbook," Jones and Bartlett, Boston, 2003.

[19] A. Heerey, M. Barry, M. Ryan and A. Kelly, "The Potential for Drug Interactions with Statin Therapy in Iraland," *Irish Journal of Medical Science*, Vol. 169, No. 3, 2001, pp. 176-179.

[20] A. J. Ellsworth, D. M. Witt, D. C. Dugdale and L. M. Oliver, "Mosby's Medical Drug Reference," 2003.

[21] R. S. Munford, "Statins & the Acute Phase Response," *New England Journal of Medicine*, Vol. 344, No. 26, June 2001, pp. 2016-2018.

[22] M. H. Shishehbor, M. L. Brennan, R. J. Aviles, X. Fu, M. S. Penn, D. L. Sprecher and S. L. Hazen, "Statins Promote Potent Systemic Antioxidant Effects Through Specific Inflammatory pathways," *Circulation*, Vol. 108, No. 4, 2003, pp. 426-431.

[23] T. Vishal, G. Bano, V. Khajuria, A. Parihar and S. Gupta, "Pleiotropic Effects of Statins," *Indian Journal Pharmacology*, Vol. 37, No. 2, 2005, pp. 77-85.

[24] M. E. Marketou, E. A. Zacharis, D. Nikitovic, E. S. Ganotakis, F. I. Parthenakis and N. Maliaraki, "Early Effects of Simvastatin Versus Atorvastatin on Oxidative Stress Proinflammatory Cytokines in Hyperlipidaemic Subjects," *Angiology*, Vol. 57, No. 2, March 2006, pp. 211-218.

[25] V. V. Uzunova, A. N. Tolekova, G. S. IIieva and A. P. Trifonova, "Renin-Angiotensin System & Lipid Peroxidation," *Bulgarian Journal of Veterinary Medicine*, Vol. 1, 2005, pp. 69-75.

[26] B. I. Kasiske, J. Z. Ma, R. S. Kalil and T. A Louis, "Effects of Antihypertensive Therapy on serum lipids," *Annals of Internal Medicine*, Vol. 122, No. 2, January 1995, pp. 133-141.

[27] N. Kebapci, B. Efe, F. Akyuz, E. Sunal and C. Demirustu, "Oxidative Stress & Antioxidant Therapy in Type 2 Diabetes Mellitus," *Turkish Journal of Endocrinology & Metabolism*, Vol. 4, 1999, pp. 153-162.

[28] G. L. Ellman, "Tissue Sulfhydyl Groups," *Archives of Biochemistry and Biophys*, Vol. 82, No. 1, May 1959, pp. 70-77.

[29] B. Guidet and S. V. Shah, *American Journal of Physiology*, Vol. 257, No. 26, 1989, p. 440.

[30] W. H. Michael, M. J. Pabst and W. B. Jakoby, "Glutathione-S-Transferase. The First Enzymatic Step in Mercapturic Acid Formation," *Journal of Biological*

Chemistry, Vol. 22, No. 25, 1974, pp. 7130-7139.

[31] H. Aebi, In Methods of Enzymatic Analysis, H.U. Bergme-tered, ed, *New York, Academic press* 1974, Vol, 2, pp. 674-678.

[32] W.T. Friedewald, R.I. Levy and D.S. Fredrickson, "Estimation of the Concentration of LDL-C in Plasma without Use the Preparative Ultracentrifuge," *Clinical Chemistry*, Vol. 18, No. 6, Jun 1972, 499-502.

[33] V. Save, N. Patil, N, Moulik and G. Rajadhyaksha, "Effect of Atorvastatin on Type 2 Diabetic Dyslipidaemia," *Journal of Cardiovascular Pharmacololgy & Therapeutics*, Vol. 11, No. 4, December 2006, pp. 262-270.

[34] M. Koter, M. Broncel, J. Chjnowska-Jezierska, K. Klikczynska and I. Franiak, "The Effect of Atorvastatin on Erythrocyte Membranes & Serum Lipids in Patients with Type 2 Hypercholesterolaemia," *European Journal of Clinical Pharmacology*, Vol. 58, No. 8, 2002, pp. 501-506.

[35] J.K. Liao and U. Laufs, "Pleiotropic Effects of Statins," *Annual Review Pharmacology & Toxicology*, Vol. 45, Febreuary 2005, pp. 89-118.

[36] J. C. Mason, "Statins & Their Role in Vascular Protection," *Clinical Science*, Vol. 105, 2003, pp. 251-266.

[37] S. Passi, A. Stancato, E. Aleo, A. Dmitrieva and G.P. Littarru, "Statins Lower Plasma & Lymphocyte Ubiquinol Ubiquinone Without Affecting Other Antioxidants & PUFA," *Biofactors*, Vol. 18, No. 1-4, 2003, 113-124.

[38] S. Wassmann, U. Laufs, K. Muller, C. Konkol, K. Ahlbory and .T. Baumer, *et al*, "Cellular Antioxidant Effects of Atorvastatin in Vitro & in Vivo," *Arteriosclerosis, Thrombosis and Vascular Biology*, Vol. 22, 2002, pp. 300-305.

[39] DALI Study Group, "The Effect of Aggressive Versus Standard Lipid Lowering by Atorvastatin on Diabetic Dyslipidaemia: the DALI Study: A double Blind Randomized Placeb Controlled Trial in Patients with Type 2 Diabetes & Diabetic Dyslipidaemia," *Diabetes Care*,Vol. 24, No. 8, 2001, pp. 1335-1341.

[40] M. Alegret and J.S. Silvestre, "Pleiotropic Effects of Statins & Related Pharmacological Experimental Approaches," *Methods and Finding Experimental Clinical Pharmacology*, Vol. 28, No.9, 2006, pp. 627.

[41] K. Sakabe, N. Fukuda, K. Wakayama, T. Nada, H. Shinohara and Y. Tamura "Effects of Atorvastatin Therapy on the Low - Density Lipoprotein Subfraction, Remnant-Like Particles Cholesterol, and Oxidized Low-Density Lipoprotein within 2 Weeks in Hypercholesterolemic Patients," *Circulation Journal*, Vol. 67, No. 10, 2003, pp. 866-870.

[42] U. Laufs and J.K. Liao, "Isoprenoid Metabolism & the Pleiotropic Effects of Statins," *Current Atherosclerosis Reports*, Vol. 5, No.5, 2003, pp. 372-378.

Pharmacology & Pharmacy, **2010, 1, 60-68**
doi:10.4236/pp.2010.12009 Published Online October 2010 (http://www.SciRP.org/journal/pp)

Structure Analysis for Hydrate Models of Ethyleneimine Oligomer by Quantum Chemical Calculation

Minoru Kobayashi[1], Hisaya Sato[2]

[1]Graduate School of Bio-Applications and Systems Engineering, Tokyo University of Agriculture and Technology, Tokyo, Japan; [2]Graduate School of Technical Management, Tokyo University of Agriculture and Technology, Tokyo, Japan.
Email: mikoba3@aol.com

Received June 14th, 2010; revised July 14th, 2010; accepted August 10th, 2010.

ABSTRACT

Structure analyses for hydrate models of ethyleneimine oligomer (5-*mer as model of PEI*) *were investigated by quantum chemical calculations. Conformation energies and structures optimized for hydrate models of* $(ttt)_5$ *and* $(tgt)_5$ *conformers were examined. Hydrate ratio, h* [*h* = H_2O/N (*mol*)], *was set from* 0.5 *to* 2. *In anhydrates,* $(tg^+t)_5$ *conformer was more stable* (−1.8 *kcal/m.u.*) *than* $(ttt)_5$. *In hydrates,* $(ttt)_5$ *conformers were more stable* (−0.7 - −4.3) *than* $(tg^+t)_5$. *These results corresponded to experimental results that anhydrous linear PEI crystal changes from double helical to single planar chain in hydration process. Structures calculated for* $(ttt)_5$ *agreed in those observed for hydrates of PEI. In all* $(tg^+t)_5$ *conformers, O···H bonds between waters were found with the decreases of N···H bonds between imino group and water. The O···H bonds in* $(tg^+t)_5$ *conformer resulted in its high chain torsion, and strongly related with instability and structure change* (*large swelling*).

Keywords*: *Structure Analysis*, *Conformation*, *Hydrate*, *Poly*(*Ethyleneimine*), *Oligomer*, *Quantum Chemical Calculation

1. Introduction

Linear poly(ethyleneimine) (PEI, $(-CH_2CH_2NH-)_n$) exhibits various kinds of crystalline phases. X-Ray diffraction (XRD) [1-3] and time-resolved infrared spectral measurement [4] have confirmed that the structure of anhydrate is a 5/1 double stranded helix with a repeating tgt (t: trans, g: gauche) conformation for N-C, C-C, and C-N bonds, and in the hydrate, the structure transforms to the planar zigzag with ttt conformation. In hydration process, the anhydrate changes to the hemi-hydrate (H_2O/EI = 0.5/1 mol), subsequently the sesqui-hydrate (H_2O/EI = 1.5/1), and finally the di-hydrate (H_2O/EI = 2/1) with increasing water contents. The mechanism of such characteristic transitions, however, is not yet clear. The understanding of the mechanism is important also in relation with the biological problem of double stranded DNA chains.

To complement the experimental observations in the conformations of PEI, computational chemistry has been employed. Analyses for anhydrate models using molecular mechanics (MM) and molecular dynamics (MD) have been reported [5,6]. Furthermore, recent studies involve quantum chemical calculations method (QCC) [7-9]. The reports concerning an analysis using hydrate model of PEI, however, seem to be little [10]. We have investigated the conformation analyses for EI oligomer models by QCC [11-12]. Most recently, for the hydrate models with various conformations $((ttt)_x$, $(ttg^+)_x$, $(tg^+t)_x$, $(tg^+g^+)_x$, $(tg^+g^-)_x$, and $(g^+g^+g^+)_x$, x: monomer units number; x = 1 – 8) of EI oligomers, we reported [13] that the $(tg^+t)_x$ and $(ttt)_x$ conformers are the most stable in anhydrate and hydrate (hydrate ratio: h (H_2O/N (mol) = 1), respectively, and the stabilities of conformers seemed to be related with hydrogen bonding between water molecules. However, the details of mechanism in such transfer from $(tg^+t)_x$ to $(ttt)_x$ were not yet clear.

In this study, in order to deepen an understanding to the mechanism of such transfer of PEI in hydration process, the structure analyses for hydrate models of EI oligomer were investigated by QCC in more detail. The 5-mer model (single chain) as PEI model was used. The conformation energies and structures of only the $(ttt)_5$ or $(tgt)_5$ conformer with various hydrate ratios were esti-

mated from the optimized structures. The conformational characteristics of hydrates were discussed, and were compared with the experimental results observed for PEI's crystals in hydration process.

2. Calculation

2.1. Designations of Anhydrate Models

For anhydrate model, EI 5-mer capped with N-methylimino and methyl group (single chain: CH_3NH-$(CH_2CH_2NH)_5$-CH_3) was used. For its conformation, the $(ttt)_5$ and $(tgt)_5$ conformers were prepared. The conformations: $(\tau_n\tau_{n+1}\tau_{n+2})_{x=5}$ (τ: dihedral angles, n: sequential number of atoms along a skeletal chain, x: monomer units number) were designated for the combination of τ that are repeated for the units of N-C, C-C, and C-N bonds. Every dihedral angle was independently assigned along the skeletal chains. The descriptive example designated for the model (EI 1-mer) as ethyleneimine monomer is given in **Figure 1**. As reported in our previous paper [11], the conformation energies optimized for anhydrate models of EI oligomers (1 - 11-mer) using QCC (by RHF/6-31 + G(d,p) basis set) affected by the designation values for the trans conformation. All the most stable conformers were obtained by using the designation values for trans as follow: $(\tau_n/\tau_{n+1}/\tau_{n+2})_x$ was $(-175^\circ/-175^\circ/180^\circ(\pi))_x$, whose pseudo-asymmetries based on a nitrogen inversion were racemo. This designation system is partially restricted system, which was defined as that restricted from π to a unidirectional angle as trans helical condition. In this study, therefore, this system was used for the designations of trans values of dihedral angle. For the $(tg^+t)_5$ conformer, $(-170^\circ/+60^\circ/180^\circ(\pi))_{x=5}$ was used as $(\tau_n/\tau_{n+1}/\tau_{n+2})_{x=5}$ value.

2.2. Designations of Hydrate Models

Hydrate models were prepared by locating water molecule near the nitrogen atom in the optimized structures for anhydrate. The optimization for anhydrate was carried out firstly using RHF/STO-3G and then RHF/6-31G basis sets. The specified models are given in **Table 1**. Hydrate ratio (h) was defined by $H_2O_{mol}/N_{mol\ in\ oligomer}$, and the values of 0.5-2 were set. Two types of models were used: in one model water molecules are attached to discontinuous monomer units (α type) and in the other to continuous monomer units (β type) as shown in **Table 1**. The structure designated for EI 1-mer as a descriptive example is given in **Figure 1**. Hydrate distance ($d_{N\text{-}H}$, (Å)) was defined by the unbonded distance between the nearest nitrogen atom (N) and hydrogen atom (H) of HOH' in which H atom is closer to the nitrogen atom than H' atom as shown in **Figure 1**. For all conformers except for the $(tg^+t)_5$ conformers with h = 1.5 and 2, the value of 1.7 Å was used as $d_{N\text{-}H}$, according to the results in our previous report [13] in which the effects of designations of $d_{N\text{-}H}$ on the optimized structures were examined to the experimental results. In the $(tg^+t)_5$ conformers with h = 1.5 and 2, the $d_{N\text{-}H}$ values of 1.7 and 5.2 Å for a di-hydrate NH unit were used in order to avoid a crowding of water molecules in designation structure. The direction effects in location of water molecule (to N or H in NH group) on the optimized structures and energies were not found.

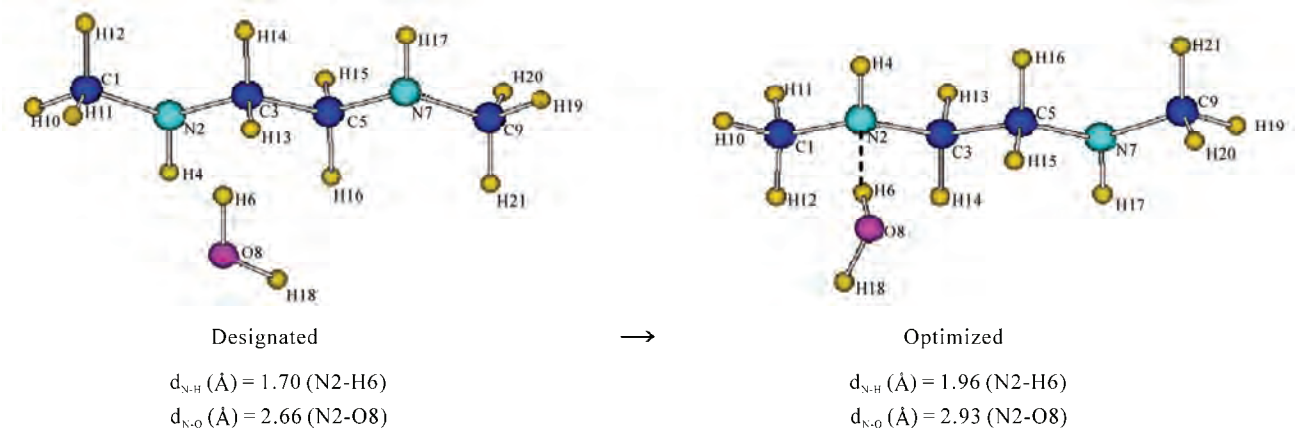

Figure 1. Descriptive examples of designated and optimized structures for hydrate model of ethylenimine monomer (EI 1-mer, conformation: $(ttt)_1$, h = 0.5, α type, (- - -: hydrogen bond). Conformation was defined by $(\tau_n\tau_{n+1}\tau_{n+2})_{x=1}$, where τ_n, τ_{n+1}, and τ_{n+2} are the dihedral angles (°) for N-C, C-C, and C-N bonds, respectively, and x is monomer unit number. In "Dseignated" of the figure, −175°, −175°, and π as the dihedral angles (τ_n, τ_{n+1}, and τ_{n+2}: partially restricted system) were used for N2-C3, C3-C5, and C5-N7 bonds, respectively. Hydrate distance ($d_{N\text{-}H}$, (Å)) was defined in hydrogen bonded NH group and water (N···H, N2-H6) as shown in "Optimized" in the figure. Conformer length was defined by L (Å), where L is unbonded distance between the terminal nitrogen atoms: N2-N7 in the figure.

Table 1. Hydrate models for ethyleneimine oligomer (EI 5-mer).

Hydrate models[1] No. Models	Hydrate type	Number of H_2O: N_w	Hydrate ratio: h (H_2O/N, mol)
1 N-N-N-N-N-N	-	0	0.000
2 N-N-N-N-N-N	α	3	0.500
3 N-N-N-N-N-N	β	3	0.500
4 N-N-N-N-N-N	β	4	0.667
5 N-N-N-N-N-N	β	5	0.833
6 N-N-N-N-N-N	β	6	1.000
7 N̆-N-N̆-N-N̆-N	β	9	1.500
8 N̆-N̆-N̆-N̆-N̆-N̆	β	12	2.000

[1]N and N̆ show the mono- and di-hydrated nitrogen units, respectively, (N = RNHR', R or R' = CH_3 or CH_2CH_2). The α and β show discontinuous and continuous hydrate units, respectively.

2.3. Structure Optimizations

Structure optimizations were carried out for each model using QCC via the Gaussian 03W (Gaussian Inc.) program [14], according to the methods in our previous report [13]. RHF/6-31G basis set was used. Gross energy of hydrated conformer with waters, E_h (Hartree, 1 Hartree = 627.51 kcal/mol), was calculated. Conformation energy of conformer, E_c (Hartree) was calculated via Equations (1) and (2),

$$E_c = E_h - \sum E_w \quad (1)$$

$$\sum E_w = E_{w(n)} + E_{w(h)} \quad (2)$$

where $\sum E_w$ is the total energy of water molecules. $E_{w(n)}$ and $E_{w(h)}$ are the energies of non-hydrogen and hydrogen bonded water molecules, respectively.

The $E_{w(n)}$ was calculated for the model of non-hydrogen bonded water molecules which are consisted of n units of single water molecule by RHF/6-31G basis set (refer **Table 2**). As the unit number (n) in the calculation of $E_{w(n)}$, the number of water molecules ($N_{w(n)}$) with non-hydrogen bonded water molecules, which was estimated in the structures optimized for the hydrate models, was used (refer **Table 4**, **Figure 2** and **Figure 3**). In the same way, the $E_{w(h)}$ was calculated for the model of linearly hydrogen bonded water molecules which are consisted of n units of sequential water molecules. As n in the calculation of $E_{w(h)}$, the number of water molecules ($N_{w(h)}$) with hydrogen bonded water molecules was used. Hydrogen bond (O···H bond) between water molecules was confirmed by the unbonded O···O distance ($d_{O\text{-}O}$) between water molecules. The $d_{O\text{-}O}$ values in non-hydrogen and hydrogen bonded water molecules were defined as the larger and smaller value than 3 Å, respectively, according to the results observed for water dimer ($d_{O\text{-}O}$: 2.74 Å in regular ice [15], 2.85 Å in liquid [15], and 2.98 Å in vapor [16,17]). The $d_{O\text{-}O}$ values in O···H bonded water molecules estimated for the models of water molecules were smaller than 3 Å. The calculated $E_{w(n)}$ and $E_{w(h)}$ values are given in **Table 2**. The examples for conformation energies (E_c) are given in **Table 3**.

Table 2. Energies (E_w, HF) calculated for water molecules by RHF/6-31G.

n[1]	$E_{w(n)}$[2]	$E_{w(h)}$[3]	n[1]	$E_{w(n)}$[2]	$E_{w(h)}$[3]
1	−75.9854	-	5	−379.9274	−379.9876
2	−151.9708	−151.9826	6	−455.9128	−455.9907
3	−227.9562	−227.9830	9	−683.8686	−684.0007
4	−303.9416	−303.9850	12	−911.8256	−912.0114

[1]Units number of water molecules. [2]Energies of non-hydrogen bonded water molecules. [3]Energies of linearly hydrogen bonded water molecules which are consisted of n units of sequential water molecules ($d_{O\text{-}O}$ calculated: 2.71 - 2.85 Å).

The conformation in optimized structure was specified based on IUPAC [18] as follow: τ_n of trans ($t^{\pm}$) and gauche ($g^{\pm}$) are from ± 120° to ± 180° and from ± 0° to ± 120°, respectively. Hydrate distance ($d_{N\text{-}H}$, (Å)) was defined as mentioned before, and its example is shown in **Figure 1**. Another parameter for hydrate distance was defined by $d_{N\text{-}O}$ (Å), where $d_{N\text{-}O}$ is unbonded distance between nitrogen atom (N) of imino group and oxygen atom (O) of neighboring water molecule. The $d_{N\text{-}O}$ value in hydrogen bonded (N···H bond) imino group/water molecule was defined as smaller value than 3 Å ($d_{N\text{-}H}$ < 2 Å) according to the results observed for hydrous PEI's crystals ($d_{N\text{-}O}$: 2.87 - 3.05 [2,3], see **Table 5**). Conformer length was defined by L (Å), where L is unbonded distance between terminal nitrogen atoms as shown in footnote of **Figure 1**. Diameter of $(tgt)_5$ conformer was defined by D (Å), where D is relative diameter which was measured as the largest value in chain axis projection for optimized structure based on D value of anhydrate.

3. Results and Discussion

3.1. Conformation Energies (Ec) Calculated for Hydrate Models of (ttt)5 and (tg+t)5 Conformers

The structures optimized for the hydrate models of $(ttt)_5$ and $(tg^+t)_5$ conformers of EI 5-mer as model of PEI were examined. In **Figures 2** and **3**, the examples of structures optimized for $(ttt)_5$ and $(tg^+t)_5$ conformers are shown, respectively. In both figures, the hydrogen bonds with

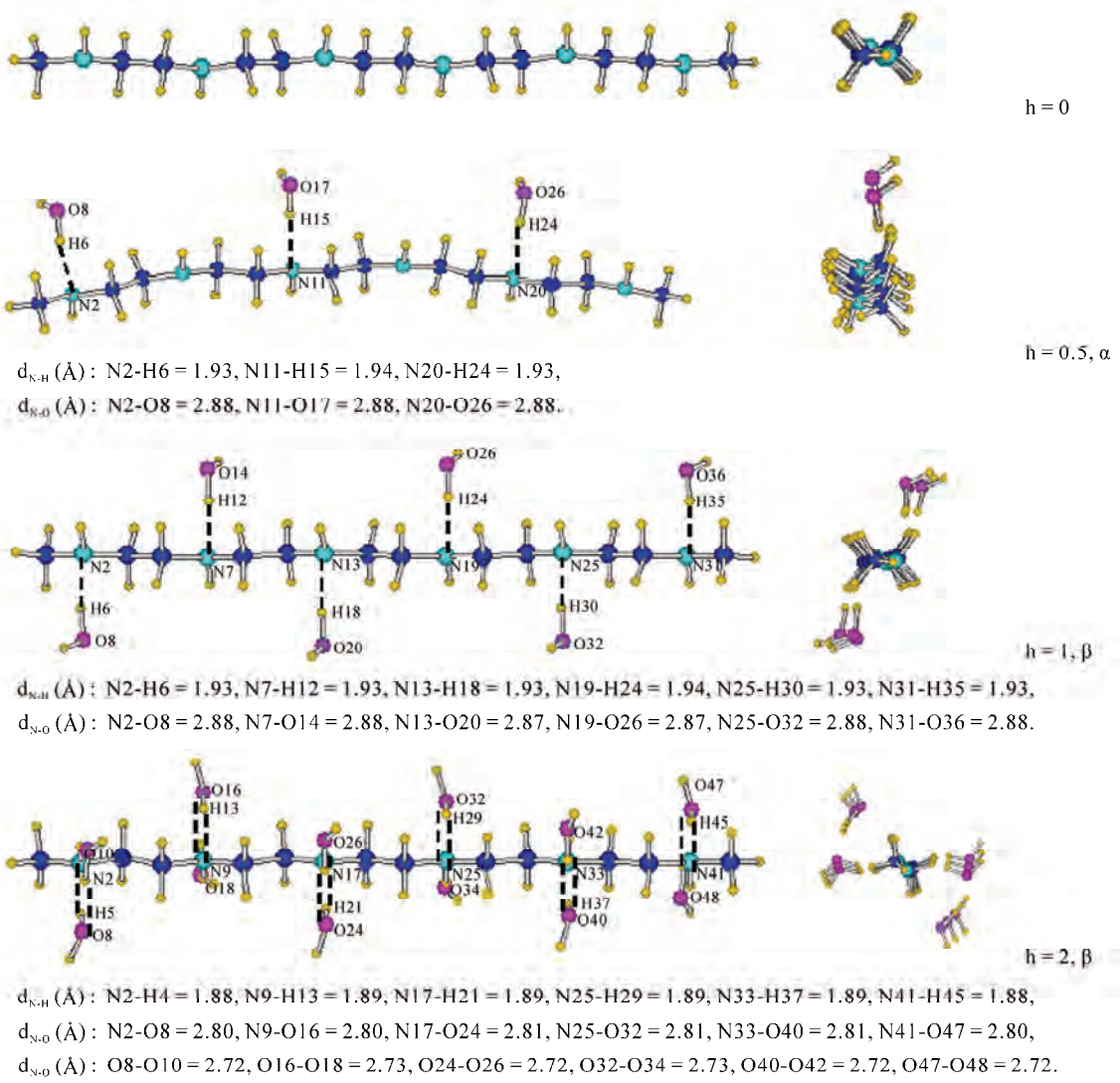

Figure 2. Structures optimized for hydrate models of $(ttt)_5$ conformer of EI 5-mer by RHF/6-31G. Left and right side figures show the stereo oblique and chain axis projections, respectively. (- - -: hydrogen bonds, d_{N-H} (d_{N-O}): unbonded distances in hydrogen bonded NH group/water, d_{O-O}: unbonded distances in hydrogen bonded water/water).

water molecules are specified as follows: the N···H bond between imino group and water molecule (N···H bond, d_{N-H} < 2 Å and d_{N-O} < 3 Å) and the O···H bond between water molecules (O···H bond, d_{O-O} < 3 Å) are shown with the d_{N-H}, d_{N-O} and d_{O-O} values. In $(ttt)_5$ conformers with h = 0.5 and 1, as shown in **Figure 2**, the hydrogen bond with water molecule is only N···H bond, and the O···H bond is nothing. The number of water molecules with N···H bond ($N_{w(h')}$) increases (3 to 6) with increases (0.5 to 1) of h values. In $(ttt)_5$ conformers with h = 2, as shown in **Figure 2**, both N···H and O···H bonds are found in each pair of imino group and water molecules, and the $N_{w(h')}$ and the number of water molecules with O···H bond ($N_{w(h)}$) are 6 and 12 (2 × 6, n = 2), respectively. On the other hand, in $(tg^+t)_5$ conformers, the N···H and O···H bonds are found in all conformers as shown in **Figure 3**. For example, in $(tg^+t)_5$ conformers with h = 0.5 (discontinuous hydrate type: α), the $N_{w(h')}$ and $N_{w(h)}$ values are 3 and 2, respectively.Å

The conformation energy (E_c) of hydrate conformer was estimated as the difference between the gross energy of hydrated conformer with waters (E_h) and the total energy of water molecules ($\sum E_w$) using Equations (1) and (2) as mentioned in previous section. The examples of conformation energies (E_c) are shown in **Table 3**. The E_c values were calculated using the number of water molecules with non-hydrogen and/or hydrogen bond ($N_{w(n)}$ and/or $N_{w(h)}$) obtained in **Figures 2** and **3**. All results are summarized in **Table 4.**

Conformation energy for the most stable hydrate con-

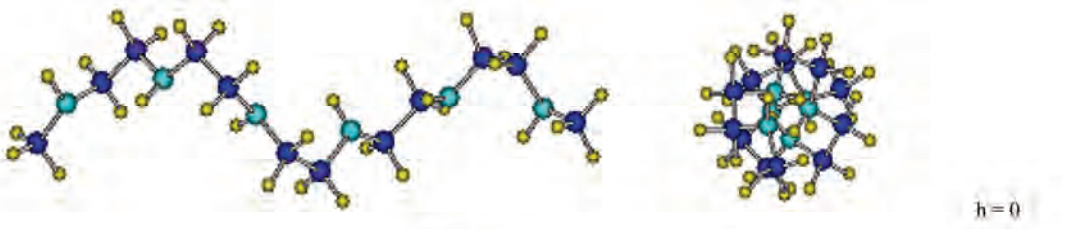

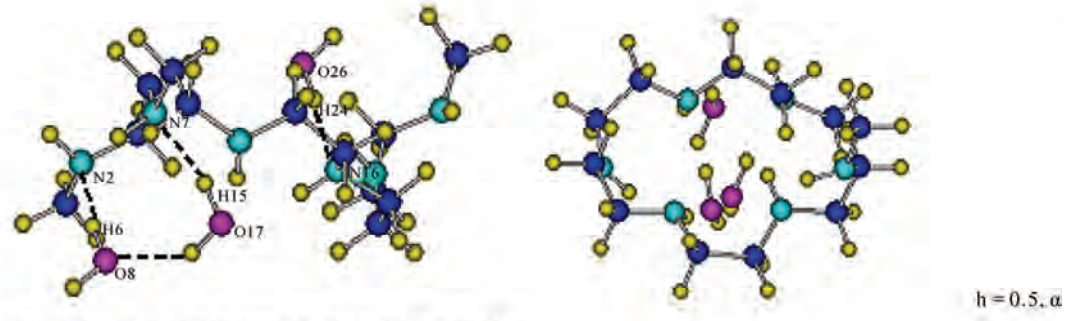

$d_{N\text{-}H}$ (Å) : N2-H6 = 1.90, N7-H15 = 1.94, N16-H24 = 1.90,
$d_{N\text{-}O}$ (Å) : N2-O8 = 2.86, N7-O17 = 2.89, N16-O26 = 2.87,
$d_{N\text{-}O}$ (Å) : O8-O17 = 2.80.

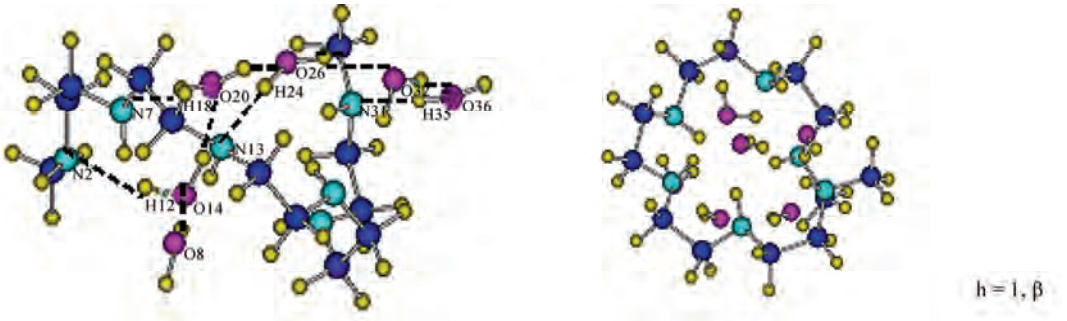

$d_{N\text{-}H}$ (Å) : N2-H12 = 2.00, N7-H18 = 1.93, N13-H24 = 1.99, N31-H35 = 1.83,
$d_{N\text{-}O}$ (Å) : N2-O14 = 2.95, N7-O20 = 2.89, N13-O26 = 2.95, N31-O36 = 2.79,
$d_{N\text{-}O}$ (Å) : O8-O14 = 2.76, O14-O20 = 2.71, O20-O26 = 2.71, O26-O32 = 2.75, O32-O36 = 2.76.

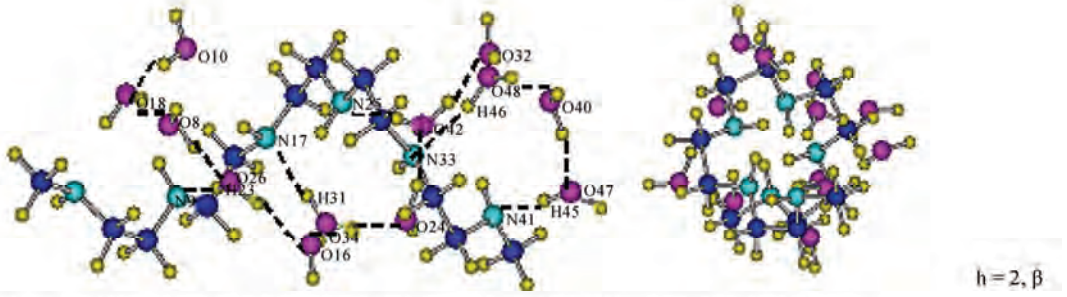

$d_{N\text{-}H}$ (Å) : N9-H23 = 1.99, N17-H31 = 1.94, N25-H39 = 1.98, N33-H46 = 2.00, N41-H45 = 1.79,
$d_{N\text{-}O}$ (Å) : N9-O26 = 2.94, N17-O34 = 2.91, N25-O42 = 2.94, N33-O48 = 2.94, N41-O47 = 2.77,
$d_{N\text{-}O}$ (Å) : O10-O18 = 2.69, O18-O8 = 2.71, O8-O26 = 2.62, O26-O16 = 2.74, O16-O34 = 2.61, O34-O24 = 2.71, O24-O42 = 2.61, O42-O32 = 2.71, O32-O48 = 2.62, O48-O40 = 2.71, O40-O47 = 2.66.

Figure 3. Structures optimized for hydrate models of $(tg^{+}t)_5$ conformer of EI 5-mer by RHF/6-31G. Left and right side figures show the stereo oblique and chain axis projections, respectively. (- - -: hydrogen bond, $d_{N\text{-}H}$ ($d_{N\text{-}O}$): unbonded distance in hydrogen bonded NH group/water, $d_{O\text{-}O}$: unbonded distance in hydrogen bonded water/water).

Table 3. Examples of conformation energies (E_c) (Model: No. 2 (h = 0.5, hydrtate type: α), by RHF/6-31G).

Conformations	E_h (HF)	Water molecules						E_c (HF)
		Number of water (N_w)[1]	Non-hydrogen bonds		Hydrogen bonds		$\sum E_w$ (HF)	
			$N_{w(n)}$[2]	$E_{w(n)}$ (HF)	$N_{w(h)}$[4]	$E_{w(h)}$ (HF)[3]		
$(ttt)_5$	−1027.2999	3	3	−227.9562	0	0	−227.9562	−799.3437
$(tg^+t)_5$	−1027.3266	3	1	−75.9854	2	−151.9826	−227.9680	−799.3586

[1]$N_w = N_{w(n)} + N_{w(h)}$. [2]Number of water molecules with non-hydrogen bond ($d_{O\text{-}O} \geq 3$ Å), obtained in **Figure 2** or **3**. [3]From **Table 2**. [4]Number of water molecules with hydrogen bond (O···H, $d_{O\text{-}O} < 3$ Å), obtained in **Figure 2** or **3**.

Table 4. Structure analyses for hydrate models of ethyleneimine oligomer (EI 5-mer) by RHF/6-31G.

	Models	No.1	No.2	No.3	No.4	No.5	No.6	No. 7	No.8
	Number of water: N_w	0	3	3	4	5	6	9	12
	Hydrate ratios: h	0	0.5 (α)	0.5 (β)	0.67 (β)	0.83 (β)	1 (β)	1.5 (β)	2 (β)
$(ttt)_5$	E_h (HF)	−799.3040	−1027.2999	−1027.2990	−1103.2996	−1179.2976	−1255.2968	−1483.3103	−1711.3289
	$N_{w(n)}$ / $N_{w(h)}$	-	3/0	3/0	4/0	5/0	6/0	3/(2 × 3)	0/(2 × 6)
	$N_{w(h')}$[1]	-	3	3	4	5	6	6	6
	$\sum E_w$ (HF)	-	−227.9562	−227.9562	−303.9416	−379.9274	−455.9128	−683.9040	−911.8956
	E_c (HF)	−799.3040	−799.3437	−799.3428	−799.3580	−799.3702	−799.3840	−799.4063	−799.4333
	ΔE_c (kcal/m.u.)[2]	0.00	−4.98	−4.87	−6.78	-8.31	-10.1	12.8	-16.2
	τ_n (°)[3]	−180.0	−179.6	179.1	−178.7	178.4	179.0	177.9	179.3
	N-H'$_{N'}$ / N'-H_N (Å)[4]	4.01/4.01	4.01/4.02	4.01/4.01	4.02/4.02	4.01/4.01	4.02/4.02	4.01/4.00	4.00/4.00
	2 mol length (Å)[5]	7.35	7.35	7.37	7.38	7.38	7.37	7.37	7.37
	L (Å)	18.38	18.31	18.41	18.42	18.43	18.44	18.42	18.44
$(tg^+t)_5$	E_h (HF)	−799.3183	−1027.3266	−1027.3299	−1103.3372	−1179.3459	−1255.3603	−1483.3851	−1711.4103
	$N_{w(n)}$ / $N_{w(h)}$	-	1/2	0/3	0/4	0/5	0/6	0/9	0/12
	$N_{w(h')}$[1]	-	3	2	3	4	4	5	5
	$\sum E_w$ (HF)	-	−227.9680	−227.9830	−303.9850	−379.9876	−455.9907	−684.0007	−912.0114
	E_c (HF)	−799.3183	−799.3586	−799.3467	−799.3522	−799.3583	−799.3696	−799.3844	−799.3989
	ΔE_c (kcal/m.u.)[2]	−1.79	−6.85	−5.36	−6.05	−6.81	−8.23	−10.1	−11.9
	τ_n (°)[3]	62.7	66.5	61.5	59.9	61.6	62.3	56.7	58.7
	N-H'$_{N'}$ / N'-H_N (Å)[4]	2.48/3.2	2.74/3.18	2.57/3.15	2.58/3.08	3.68/3.12	2.69/3.17	2.61/2.98	2.54/3.02
	5 mol length (Å)[5]	13.90	7.82	13.44	12.07	12.09	6.91	10.10	11.30
	L (Å)	13.57	8.66	12.93	11.84	11.93	6.99	10.81	11.59
	D (Å)	1.0	1.94	1.23	1.57	1.57	1.91	1.60	1.43

[1]Number of water molecules with hydrogen bond (N···H, $d_{N\text{-}H} < 2$ Å and $d_{N\text{-}O} < 3$ Å) between imino group and water. [2]Based on E_c of $(ttt)_5$ conformer with h = 0. [3]Average of dihedral angles for C-C bonds. [4]N-H'$_{N'}$ (or N'-H_N) is average of unbonded distance between N of NH group and H' of neighboring N'H' group (or between N' and H). [5]Average value.

former will be defined as the smallest value of the summation of anhydrate energy and hydration stability energy [19]. The hydration stability energy (ΔE_c, kcal/m.u., m.u.: monomer unit) is given as the difference between

Table 5. Comparison between the calculated and observed structures.

	Calculated for hydrate models of $(ttt)_5$ conformer			Observed for hydrous linear PEI crystals (by XRD [2,3])		
				Hemi-hydrate [2]	Sesqui-hydrate [3]	Di-hydrate [3]
	h = 0.5 (α)	h = 1.5 (β)	h = 2 (β)	h' = 0.5[1]	h' = 1.5[1]	h' = 2[1]
Conformation	all trans	all trans	all trans	all trans	all trans	all trans
2 mol length (Å)	7.35	7.37	7.37	7.31[2]	7.36[2]	7.36[2]
$d_{N\text{-}O}$ (Å)	2.88	2.87	2.81	3.05($N_a\cdots O_1$)	2.96($N_a\cdots O_1$)	2.93($N_a\cdots O_1$)
				2.87($N_a\cdots O_1$)	2.93($N\cdots O_3$)	
$d_{O\text{-}O}$ (Å)	-[3]	2.72	2.81	-[3]	2.87($O_1\cdots O_2$)	2.66($O_1\cdots O_2$)
				-[3]	2.80 ($O_1\cdots O_3$)	
				-[3]	2.79($O_1\cdots O_4$)	2.75($O_1\cdots O_4$)

[1]h': H_2O/EI (mol) [2]Fiber period, corresponding to 2 mol length. [3]Hydrogen bondings between water molecules were not estimated or observed.

the E_c values of anhydrate and hydrate. The results are shown in **Table 4**. In **Figure 4**, the relations between ΔE_c and h values are shown. The ΔE_c values decreased linearly with increases of water contents. In **Figure 5**, the $N_{w(h')}$ values (with N···H bond) are plotted against hydrate ratios (h). The $N_{w(h')}$ values increase with increases of h values until h = 1 ($(ttt)_5$) or 1.5 ($(tg^+t)_5$). These results indicate that the conformers are stabilized by an electrostatic effect of N···H bond.

In $(ttt)_5$ conformers, as shown in **Figure 4**, the ΔE_c values of two conformers with h = 0.5 of α and β (continuous) hydrate type, which have the same value (3) of $N_{w(h')}$ (**Figure 5**), are almost the same. This result indicates that the chain torsion effects on ΔE_c in $(ttt)_5$ conformers seem to be little because of the long distance between neighboring NH groups in stretched trans structure (N-H'$_N$, or N'-H_N: 4.01 Å, see **Table 4**). Although the $N_{w(h')}$ values of $(ttt)_5$ conformers with h = 1.5 and 2 are the same (6) as that with h = 1 (**Figure 5**), the ΔE_c values of the formers are smaller than that of the latter(**Figure 4**). It seems to be related with the results that the pairs of water molecules at h = 1.5 or 2 are located in series to each NH group with O···H bonds as shown in **Figure 2**.

In $(tg^+t)_5$ conformers, as shown in **Figure 4**, the plots of ΔE_c against h values show linear relation and the conformers are stabilized by hydration as same as in $(ttt)_5$ conformers. However, ΔE_c values in h over 0.5 are larger than those of $(ttt)_5$ conformers. From an energy aspect, this result corresponds to the experimental results observed for linear PEI's crystals in hydration process. The instability of $(tg^+t)_5$ conformers seems to be related with both the increases of O···H bonds and the decreases of N···H bonds. In $(tg^+t)_5$ conformers, the $N_{w(h)}$ values with O···H bond increased with increases of h values as shown in **Figure 3** and **Table 4**. And at the same time, the $N_{w(h')}$

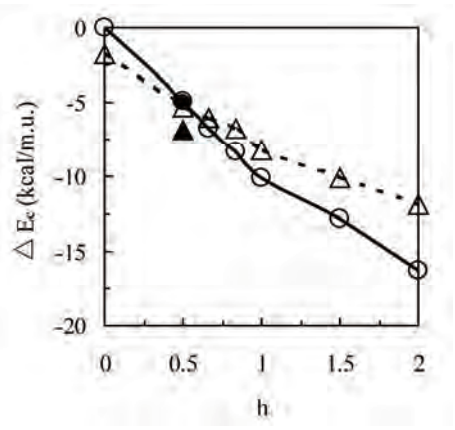

Figure 4. Plots of hydration stability energy (ΔE_c, kcal/m.u.) against hydrate ratios (h). The ● and ○ symbols show $(ttt)_5$ conformers with α and β type, respectively. ▲ and △ show $(tg^+t)_5$ conformers with α and β type, respectively.

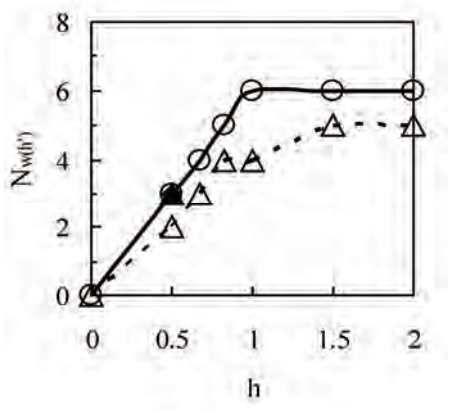

Figure 5. Plots of $N_{w(h')}$ against hydrate ratios (h). The ● and ○ symbols show $(ttt)_5$ conformers with α and β type, respectively. The ▲ and △ symbols show $(tg^+t)_5$ conformers with α and β type, respectively.

values with N···H bond are smaller than those of $(ttt)_5$ conformers as shown in **Figure 5**. As shown in **Table 4**, the N···H bond distances (N-H'$_N$, or N'-H_N) in neighboring NH groups of anhydrated $(tg^+t)_5$ conformer are smaller (0.7 - 1.2 Å) than those of $(ttt)_5$ conformer. Anhydrous PEI's chain (tgt) is strongly twisted by intra- and inter-molecular interactions (N···H bonding between imino groups). Taking into account of these results, the water molecules coming near to NH groups of $(tg^+t)_5$ conformer must strongly prefer to having a pair with O···H bonds between water molecules compared with $(ttt)_5$ conformer. For examples in h = 0.5, as shown in **Table 4**, the $N_{w(h)}$ values of $(tg^+t)_5$ conformers with α and β type are larger (2-3) than those of $(ttt)_5$ conformers with α and β type. Furthermore, the $N_{w(h)}$ value of $(tg^+t)_5$ conformer with β type is larger (1) than that with α type.

3.2. Structures Calculated for Hydrate Models of (ttt)5 and (tg+t)5 Conformers

In $(ttt)_5$ conformers, as shown in **Figure 2** and **Table 4**, the structure changes by hydrations are little. It seems to be related with the results that the effects of O···H bonds between water molecules on the structures are negligible. The O···H bonds were not found in conformers with h ≤ 1, but were found in the conformers with h = 1.5 and 2. In h = 1.5 and 2, the O···H bonds are independent in each hydrate unit (refer **Figure 2**).

In **Table 5**, the structures calculated for $(ttt)_5$ conformers were compared with those observed for linear hydrous PEI's crystals by XRD [2,3]. The 2 mol length or d_{N-O} value calculated for the conformers with h = 0.5 (α, β type), 1.5 and 2 agreed in that observed for hemi-(H_2O/EI, mol = 0.5) [2], sesqui- (1.5) [3] and di-hydrate (2) [3], respectively. The results that the O···H bonds between water molecules were not found in the conformers with h = 0.5 (α and β type) corresponded to the experimental results observed for hemi-hydrate as shown in **Table 5**. The d_{O-O} values calculated for the O···H bonded water molecules in conformers with h = 1.5 and 2 agreed in those observed for sesqui- [3] and di-hydrate [3]. These agreements in the calculated and observed results should be noticed. Polymer chains in hydrous crystal are separated to a single chain (ttt) with hydrogen bonded water molecule (N···H and/or O···H bond). The structures calculated for single chain models will be fundamentally different from those observed for hydrous polymer crystals. These agreements seem to be resulted in "a single chain" in both cases.

As shown in **Figure 3**, the structure calculated for anhydrate model of $(tg^+t)_5$ conformer fundamentally corresponded to the structure observed for anhydrous linear PEI's crystal (5/1 double stranded helix, tgt [1]). However, the 5 mol length calculated (13.90 Å, in **Table 4**) was different from that observed (9.58 Å [1]). This difference indicates that the double stranded helical chains of PEI are largely shrinking and swelling because of their inter-molecular interactions. The structures calculated for hydrate models of $(tg^+t)_5$ conformer largely changed by hydrations as shown in **Figure 3** and **Table 4**. The plots of shrinkage rates ($\Delta L/L_0$ (%), L_0: conformer length calculated for anhydrate) against h values are shown in **Figure 6**. In **Figure 7**, the swelling rates in $(tg^+t)_5$ conformers ($\Delta D/D_0$ (%), D_0: diameter calculated for anhydrate) are plotted against h values. As shown in **Figures 6** and **7**, the $(tg^+t)_5$ conformers with h = 0.5 (α type) and 1 (β type) are strongly shrinking and swelling. It seems to be connected with the results that the water molecules with O···H bonds are located in the insides of conformers as shown in **Figure 3**. Taking into account with the results of ΔE_c (**Figure 4**), the strong swelling in $(tg^+t)_5$

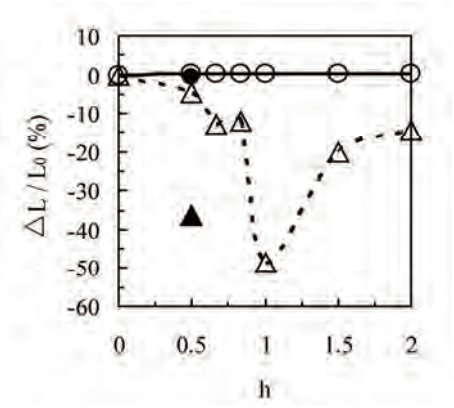

Figure 6. Plots of chain shrinkage rates ($\Delta L/L_0$ (%), ΔL: L - L_0, L_0: L of anhydrate) against hydrate ratios (h). The ● and ○ symbols show $(ttt)_5$ conformers with α and β type, respectively. The ▲ and △ symbols show $(tg^+t)_5$ conformers with α and β type, respectively.

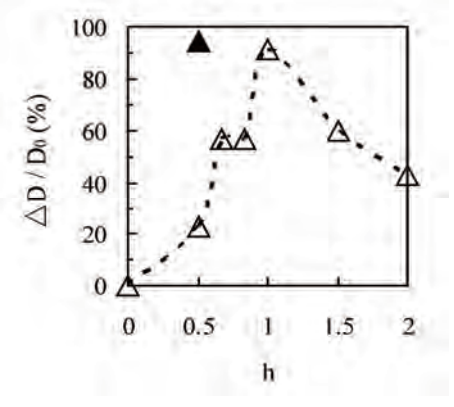

Figure 7. Plots of chain swelling rates ($\Delta D/D_0$ (%), ΔD: D - D_0, D_0: D of anhydrate) against hydrate ratios (h) in $(tg^+t)_5$ conformers. The ▲ and △ symbols show α and β type, respectively.

conformers with h values over 0.5 may be one of the driving forces for dissociation from a double helical chain to a single planar chain of PEI's crystal or other polymer chains as DNA in hydration process.

4. Conclusions

Structure analyses for hydrate models of EI 5-mer as a PEI's model were investigated by QCC. In anhydrates, $(tg^+t)_5$ conformer was more stable than $(ttt)_5$ conformer. In hydrates with hydrate ratios (h) over 0.5, $(ttt)_5$ conformers were more stable than $(tg^+t)_5$ conformers with increases of h values. From an aspect of conformation energy, these results corresponded to the experimental results that the structure of anhydrous linear PEI's crystal changes from helix (tgt) to planar zigzag (ttt) in hydration process. Structures calculated for hydrates of $(ttt)_5$ conformers agreed in those observed for hydrous PEI crystals. The instabilities (higher E_c) and structure changes (swelling) which were estimated for $(tg^+t)_5$ conformers with hydrate ratios over 0.5 were strongly connected with the formation of O···H bonds between water molecules affected by the chain torsion, and may be one of the driving forces for the dissociation of double helical chains of PEI in hydration process.

REFERENCES

[1] Y. Chatani, T. Kobatake, H. Tadokoro and R. Tanaka, "Structure Studies of Poly(ethyleneimine). 2. Double-Stranded Helical Chain in the Anhydrate," *Macromolecules*, Vol. 15, No. 1, 1982, pp. 170-176.

[2] Y. Chatani, T. Kobatake and H. Tadokoro, "Structure Studies of Poly(ethyleneimine). 3. Structural Characterization of Anhydrous and Hydrous States and Crystal Structure of the Hemihydrate," *Macromolecules*, Vol. 16, No. 2, 1983, pp. 199-204.

[3] Y. Chatani, H. Tadokoro, T. Saegusa and H. Ikeda, "Structure Studies of Poly(ethyleneimine). 1. Structures of Two Hydrates of Poly(ethyleneimine): Sesquihydrate and Dihydrate," *Macromolecules*, Vol. 14, No. 2, 1981, pp. 315-321.

[4] T. Hashida, K. Tashiro, S. Aoshima and Y. Inaki, "Structural Investigation on Water-Induced Phase Transitions of Poly(ethyleneimine). 1. Time-Resolved Infrared Spectral Measurements in the Hydration Process," *Macromolecules*, Vol. 35, No. 11, 2002, pp. 4330-4336.

[5] H. Dong, J. K. Hyun, C. Durham and R. A. Wheeler, "Molecular Dynamics Simulations and Poly(ethyleneimine) Models," *Polymer*, Vol. 42, No. 18, 2001, pp. 7809-7817.

[6] S. Wang, L. DeBolt and J. E. Mark, "Configurational Analysis of Linear Poly(ethyleneimine)," *Polymeric Preprints*, Vol. 34, No. 2, 1993, pp. 478-479.

[7] S. E. Boesch, S. S. York, R. Frech and R. A. Wheeler, "An Experimental and Computational Investigation of the Structure and Vibrations of Dimethylethylenediamine, a Model for Poly(ethyleneimine)," *PhysChemComm*, Vol. 4, 2001, pp. 1-10.

[8] Y. Sasanuma, S. Hattori, S. Imazu, S. Ikeda, T. Kaizuka, T. Iijima, M. Sawanobori, M. A. Azam, R. V. Law and J. H. G. Steinke, "Conformational Analysis of Poly(ethyleneimine) and its Model Compounds: Rotational and Inversional Isomerizations and Intramolecular and Intermolecular Hydrogen Bonds," *Macromolecules*, Vol. 37, No. 24, 2004, pp. 9169-9183.

[9] H. Kusanagi, "Quantum Chemical Examination on the Double-Stranded Helix Models of Poly(ethyleneimine)," *Polymer Preprints Japan*, Vol. 53, No. 2, 2004, pp. 3610-3611.

[10] D. Diabate, A. Yapo, A. Trokourey, A. Kone and B. Fahys, "Study of Structural and Electronic Properties of Polyethylenimine Hemihydrate," *Physical and Chemical News*, Vol. 37, 2007, pp. 122-126.

[11] M. Kobayashi and H. Sato, "Conformational Analysis of Ethylene Oxide and Ethylene Imine Oligomers by Quantum Chemical Calculation," *Polymer Journal*, Vol. 40, No. 4, 2008, pp. 343-349.

[12] M. Kobayashi and H. Sato, "Conformational Analysis of Ethylene Oxide and Ethylene Imine Oligomers by Quantum Chemical Calculations: Solvent Effects," *Polymer Bulletin*, Vol. 61, No. 4, 2008, pp. 529-540.

[13] M. Kobayashi, M. Takahashi and H. Sato, "Conformational Analysis for Hydrated Ethylene Imine Oligomer Models by Quantum Chemical Calculations," *Polymer Journal*, Vol. 41, No. 10, 2009, pp. 880-887.

[14] Gaussian Inc., "Gaussian 03 User's Reference," Gaussian Inc., Pennsylvania, 2003.

[15] R. Ludwig, "Water from Clusters to the Bulk," *Angewandte Chemie International Edition*, Vol. 40, No. 10, 2001, pp. 1808-1827.

[16] T. R. Dyke, K. M. Mack and J. S, Muenter, *J. Chem. Phys.*, Vol. 66, 1977, pp. 498.

[17] J. A. Odutola and T. R. Dyke, "Nitric Acid and Carboxylic Acid Dimers," *Journal of Chemical Physics*, Vol. 72, 1980, pp. 50-62.

[18] D. R. Lide, "CRC Handbook of Chemistry and Physics," 82nd Edition, CRC Press, London, 2001.

[19] M. Kinoshita, Y. Okamoto and F. Hirata, "Solvent Effects on Formation of Tertiary Structure of Protein," *Biophysical Society of Japan*, Vol. 40, No. 6, 2000, pp. 374-378.

Pharmacology & Pharmacy, **2010, 1, 69-74**
doi:10.4236/pp.2010.12010 Published Online October 2010 (http://www.SciRP.org/journal/pp)

The Study of Influence of Silica and Polyethilene Glycols Organic-Inorganic Compounds on Free-Radical Processes *in Vitro*

Olga G. Sitnikova[1], Sergey B. Nazarov[1], Irina V. Shikhanova[2], Alexander V. Agafonov[2], Jean A. Dyuzhev[1], Irina G. Popova[1]

[1]Ivanovo State Research Institute of Maternity and Childhood (RIMC), Ivanovo, Russia; [2]Institute of Solution Chemistry, Russian Academy of Sciences, Ivanovo, Russia.
Email: ivgenlab@gmail.com

Received July 20th, 2010; revised August 10th, 2010; accepted September 30th, 2010.

ABSTRACT

In this study investigation of influence of hybrid nanosilica-polyethylene glycols materials (*molecular weight* 1500, 6000 *and* 15000), *prepared by sol-gel synthesis, on lipid peroxidation and antioxidant activity of human serum in vitro was performed. Methods included chemiluminescence analysis and quantitative malonic dialdehyde estimation. It was revealed that nanosilica-PEG materials with different molecular weight had certain biological activity. Powders of* SiO_2*-PEG* 1500 *and* SiO_2*-PEG* 6000 *manifest prooxidant effects, whereas mesoporous* (*calcine*) *powders produced antioxidant effects in blood serum in vitro.*

Keywords*: *Free-Radical Oxidation, Nanosilica, Chemiluminescence, Malonic Dialdehyde

1. Introduction

The study of free-radical processes of lipid oxidation and antioxidant system is an important problem of modern biomedicine. Oxygen is a powerful oxidant and oxygen-mediated reactions are the main sources of energy for variety of biological species. Metabolic processes produce reactive oxygen species (ROSs), free radicals, peroxides, malonic dialdehyde, Schiff's bases, which damage membrane structures and lead to oxidative stress, being the causative factor for a lot of widely spread diseases, including reproductive disorders and prenatal injuries [1-3].

Concerning this the role of antioxidants is to neutralize toxic products of free-radical lipid peroxidation. In conditions of excessive peroxidation the capacity of antioxidant defense may decrease due to insufficient endogenic antioxidant production or unfavorable environment factors [3]. Various substances are known to have antioxidant activity; their investigation is of certain importance for both biology and medicine [4].

Nowadays silica compounds attract considerable attention. Silica stimulates fibroblastic activity of mesenchyma, promoting granulation and scarring. The lack of silica may lead to depression of leukocyte activity in inflammation, poor wound scarring, anorexia, pruritus, tissue flexibility decrease, skin turgor decrease, vascular permeability increase and haemorrhagia as a result. Apart from this silica antioxidant activity stands [5].

Investigators of peroxidation showed that silica powders stimulated active oxygen species and free radicals production in culture of epithelial cells, resulting in caspase activation and apoptosis [6]. Some authors experimentally found out that inhalation of crystalloid silica in animals lead to oxidative stress, inflammation and alveolar fibrosis [7,8].

As a catalysts and functional composite materials special attention is attracted by matrix hybrid silica derivates. In this study we presented physical-chemical properties of silica-based materials and their influence on peroxidation processes in human serum. Silica nanoparticles are biologically inert, have high adsorption rate, thermal and mechanic stability, and therefore are expected to manifest antioxidant activity.

The aim of the work was to study the influence of organic-innorganic silica and polyethylene glycols compounds on free-radical processes *in vitro*.

2. Materials and Methods

2.1. Reagents for Silica Nanoparticles Synthesis

Tetraethoxysilane (TEOS) $(C_2H_5O)_4Si$ (high purity grade, Ekos-1, Russia), diethylamine $(C_2H_5)_2NH$ (moderate purity grade, Aldrich), polyethylene glycols $[-OCH_2CH_2-]_n$ with molecular weight of 1500, 6000, 15000 (Aldrich) and rectified ethanol (96 wt%) were used without further purification.

2.2. Synthesis of Hybrid Organic-Inorganic SiO_2-Polyethylene Glycol Materials

The synthesis was carried out in ethanol media at temperature of 20℃. Polyethylene glycol was dissolved in required amount of water and was added to ethanol. Than a catalyst of tatraethoxysilane hydrolysis – diethyl amine – was added. The resulting mixture was homogenized for 15 min. After that small doses of tatraethoxysilane (0.5-1.0 ml) were injected into the system using syringe. Total synthesis time was 17 hrs. Particles were filtered from the original solution and dried out on open air at temperature of 70-100℃ until mass stability.

We investigated two types of hybrid organic-inorganic SiO_2-PEG materials: noncalcine and calcine in muffle furnace (800℃, 2 hrs).

2.3. IR Spectroscopy

IR spectra of produced powders were recorded using Avatar 360 FT-IR ESP spectrometer (wave range: 400-4000 cm^{-1}). Preliminary samples of powders were grinded with KBr in agate mortar and pressed in discs.

2.4. Thermogravimetry

Thermogravimetric measuring were performed on thermoanalythical installation. The mass of a sample was 80-90 mg. The heating was carried out from room temperature up to 1000℃ with rate of 5℃ per min.

2.5. Brunauer-Emmett-Teller (BET) Surface Area Measurement

First step of BET analysis was heating of samples to eliminate adsorbed impurities. Then argon at temperature of 77K was adsorbed on materials to form a monomolecular film on accessible area. The amount of adsorbed argon served to determine the BET surface area.

In experiments we used native serum of 10 patients, administered in obstetrical or gynecological clinics of Ivanovo Research Institute of Maternity and Childhood. We decided not to use whole blood to prevent coagulation. Suspension of studied powders was added to 1 ml of native serum, which was then incubated at 4℃ for 1 hr. The ratio between powders and serum was 5.0 g/L for mesostructured (noncalcine) powder and 50.0 g/L for mesoporous (calcine) powder. At this stage of experiments we didn't try to evaluate pharmacological doses of studied powders as the only aim of experiments was to determine any possible pro- or antioxidant properties of synthesized materials *in vitro*. The incubation temperature was found to limit bacterial activity. Native serum without nanomaterials stood for control. After incubation samples were centrifuged at 3000 rpm for 10 min. Supernatants were transferred into clean dry tubes and underwent analysis.

2.6. Estimation of Peroxidation Intensity by Induced Chemiluminescence (CL)

The method was based on catalytic reduction of peroxides by bivalent ferric ions. Generated free radicals acted as oxidation initiators in biological substrate. Free radicals recombination followed by photon release, which could be registered in 40 s. This was a period of maximal intensity. We used hydrogen peroxide and ferric sulfate as biochemiluminescence inductors. 0.1 ml of serum was mixed with 0.4 ml phosphate buffer (pH 7.5), 0.4 ml ferric sulfate (0.01 mM), 0.2 ml 2% hydrogen peroxide and underwent CL. Intensity of luminescence was evaluated by BHL-06M biochemiluminometer (Russia). Registered parameters were as follows (**Figure 1**): peak intensity of luminescense (I_{max}) – the highest intensity of luminescense registered within first 40 seconds of Fenton's reaction; light sum (S) – the area under the curve of luminescent signal; slope of the curve (tg α) – tangent of decrease signal angle.

Imax and S reflected potential for lipid peroxidation. Antioxidant activity was characterized by tg α and coefficient K (I_{max}/S ratio).

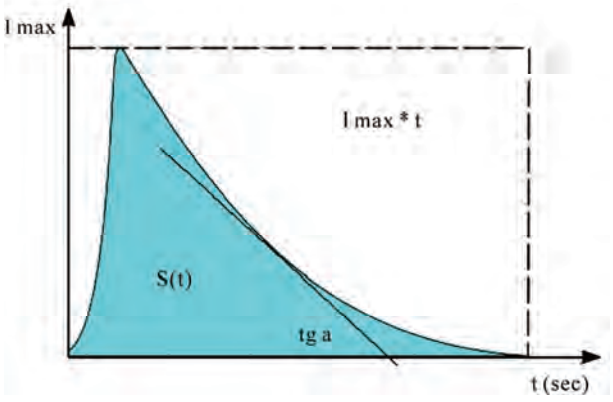

Figure 1. Typical kinetics of serum chemiluminescense. The registered parameters are as follows: peak intensity (I_{max}), light sum (S(t)), the slope of the curve (tg *α*).

2.7. Malonic Dialdehyde Serum Concentration Measurement

The method was based on reaction between malonic dialdehyde (MDA) and thiobarbituric acid [9]; the product of reaction had pink color and was identified by SF-46 spectrophotometer (Russia) on wave length 523 nm.

3. Results and Discussion

Qualitative and quantitative structure of materials was investigated by IR spectroscopy and thermogravimetric analysis.

Thermograms of hybrid organic-inorganic SiO_2-PEG material (molecular weight 15000) are presented on **Figure 2**.

Burning of polymer component from matrix SiO_2-PEG 15000 hybrid is described by the peak with maximum at 291℃ on differential thermogravimetric diagram. The amount of organic phase was 39 wt% in sample. Water content was 13.5 wt%. The curve of differential thermal analysis did not reveal any thermal effects.

Figure 3 shows IR spectra of hybrid organic-inorganic (a) SiO_2-PEG 15000 and (b) material calcined at 800℃.

There were characteristic oscillations of Si-OH and Si-O-Si found in spectra. Also, in areas of wavenumbers 3600-3500, 1640 and 400-200 cm^{-1} oscillations of adsorbed H2O, isolated and linked OH groups were found.

In spectrum of hybrid organic-inorganic SiO_2-PEG 15000 oscillations of alkyl CH_3, CH_2 and CH groups [10-19] proved the presence of organic phase in composite.

Intensive flat halo on X-ray diagram of hybrid SiO_2-PEG 15000 material reflected its amorphism (**Figure 4**).

Results of sedimentation gave data on morphology of hybrid material powders. Sizes of particles of hybrid SiO_2-PEG composite determined by sedimentation before and after calcining were (**Figure 5**) as follows. Hybrid material: 2-300 μm, with the prevalence of 24 and 150 μm fractions; tempered material: 2-110 μm, with modal size 28 μm. Specific areas of noncalcine and calcine hybrid organic-inorganic SiO_2-PEG 15000 material powders were discovered by thermal desorption of argon (**Table 1**).

Thus, there were synthesized two groups of composite materials with different structure: organic-inorganic compounds with amorphous structure and mesostructural materials with system of ordered mesochannels, filled by molecular organic templates. All materials were calcined at 800℃ for creating of high-porous silica specimens with the same structural features as their noncalcine ancestors. Investigation of pro- and antioxidant properties

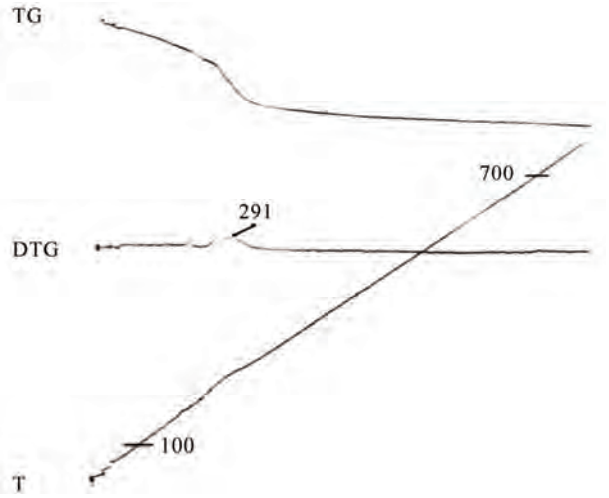

Figure 2. Thermograms of hybrid organic-inorganic SiO_2-PEG 15000 material.

Table 1. Specific surface areas of hybrid SiO2-PEG 15000 and calcined at 800℃ materials.

Material	Specific surface area by BET, m^2/g
SiO_2-PEG 15000 (noncalcine)	91
SiO_2-PEG 15000 (calcine)	> 800

of these powders was carried out *in vitro*.

Biochemical study revealed different influence of investigated powders on intensity of peroxidation in human serum (**Tables 2** and **3**). Parameters of chemiluminescence revealed in native serum were estimated as 100%.

Adding of SiO_2-PEG powders with molecular weight 1500 and 6000 to experimental system lead to increased chemiluminescence, which proved high ROS and free radical (R-, OH-, RO-, RO_2-, O_2-) production in Fenton's reaction [20,21]. Recombination of radicals formed unstable tetraoxide, which disintegrated with photon emission and raised lightsum S (plus 23%, $p = 0.0081$ and 18%, $p = 0.0131$, comparing with controls, respectively for 1500 and 6000 powders), fast flash I_{max} (plus 26%, $p = 0.0459$ for 1500 powder). Investigation of SiO_2-PEG with molecular weight 15000 didn't reveal any significant CL changes. Study of mesoporous (calcine) SiO_2-PEG powder revealed its antioxidant activity, which was developed by decreasing of peroxidation processes intensity in Samples 3 and 5 (**Table 3**). We found increasing of tg α (plus 15%, $p = 0.0510$) and decreasing of MDA. The conclusion was that nanosilica-PEG compounds with different molecular weight possessed specific oxidant and antioxidant activity. SiO_2-PEG 1500 and SiO_2-PEG 6000 powders lead to activation of free-radical oxidation,

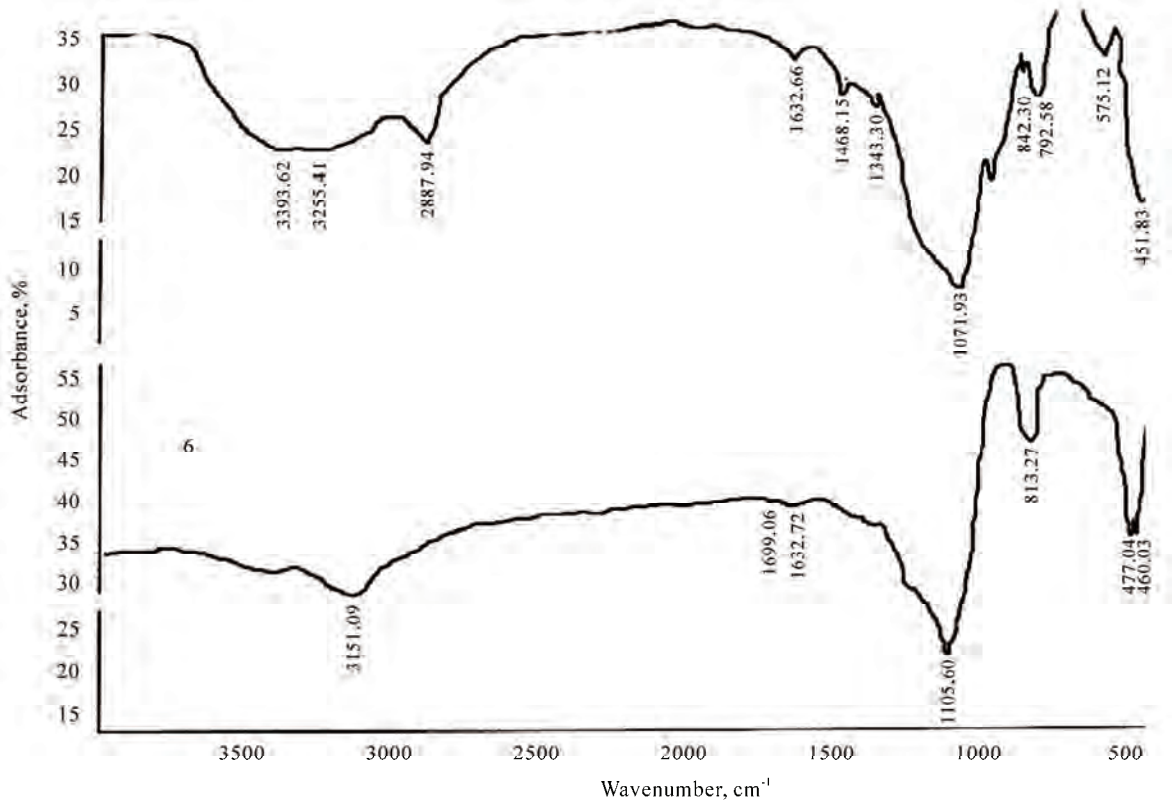

Figure 3. IR spectra of noncalcine (a) and calcine (b) hybrid organic-inorganic SiO2-PEG 15000 materials.

Table 2. Parameters of peroxidation (MDA) and induced chemiluminescence in blood serum after adding of mesostructured (noncalcine) SiO_2-PEG powders (5 mg/mL) with different molecular weight (M).

Parameters	Statistics n = 5	M=1500	M=6000	M=15000
MDA, %	M ± m	102.67 ± 21.40	86.67 ± 8.69	98.33 ± 10.81
S, %	M ± m	123.00 ± 2.08**	118.00 ± 2.08**	102.0 ± 8.39
I_{max}, %	M ± m	126.00 ± 5.77*	115.33 ± 8.69	105.33 ± 10.91
tg α, %	M ± m	125.67 ± 6.77	110.33 ± 4.06	103.00 ± 13.20
K, %	M ± m	95.67 ± 4.48	92.33 ± 4.33	97.33 ± 3.38

Note: Here and further asterix reflects significant differences among estimated groups (*p < 0,05; **p < 0,01).

Table 3. Parameters of peroxidation (MDA) and induced chemiluminescence of blood serum after adding of mesoporous (calcine) SiO_2-PEG powders (50 mg/mL) with different molecular weight (M).

Parameters	Statistics n = 5	M = 1500		M = 6000		M = 15000	
		1	2	3	4	5	6
MDA, %	M ± m	94.60 ± 9.49	86.60 ± 6.98	89.00 ± 7.77	93.20 ± 10.54	89.60 ± 3.79*	100.20 ± 4.10
S, %	M ± m	97.80 ± 3.69	93,00 ± 6.89	103.80 ± 3.62	98.40 ± 6.27	96.10 ± 1.91	109.80 ± 5.19
I_{max}, %	M ± m	104.80 ± 5.80	103.00 ± 8.96	111.20 ± 8.73	103,40 ± 12.86	98.20 ± 7.68	150.50 ± 29.70
tg α, %	M ± m	116,80 ± 9.73	128.60 ± 15.41	115.20 ± 5.17*	114.20 ± 17.11	112.80 ± 4.64*	173.25 ± 43.16
K, %	M ± m	100,40 ± 2.79	109.00 ± 2.65*	99.20 ± 1.83	99.60 ± 6.02	94.20 ± 2.48	120.00 ± 22.76

Note: Numbers 1, 2, 3, 4, 5, 6 stands for different preparations of mesoporous (calcine) SiO_2-PEG with different molecular weight (1500, 6000, 15000).

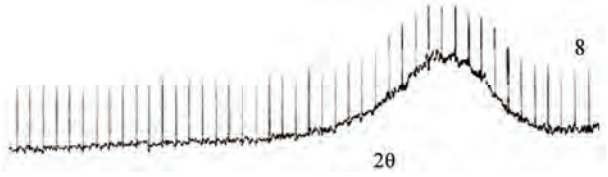

Figure 4. X-ray diagram of hybrid organic-inorganic SiO_2-PEG 15000 material.

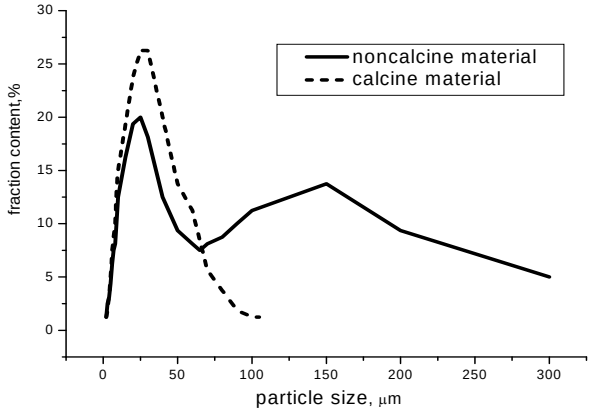

Figure 5. Particle size distribution in noncalcine and calcine hybrid organic-inorganic SiO_2-PEG 15000 materials.

whereas mesoporous (calcine) materials with molecular mass 6000 and 15000 manifested antioxidant properties in human serum due to their large specific surface area (> 800 m^2/g). These findings can be useful for creating of pharmacological preparations.

REFERENCES

[1] V. Z. Lankin, A. K. Tikhadze and Y. N. Belenkov, "Free-Radical Processes in Cardiovascular Diseases," *Kardiologiya*, Vol. 40, No. 7, 2000, pp. 48-61. (in Russian).

[2] J. Fujii, Y. Iuchi and F. Okada, "Fundamental Roles of Reactive Oxygen Species and Protective Mechanisms in the Female Reproductive System," *Reproductive Biology and Endocrinology*, No. 3, 2005, p. 43.

[3] V. A. Terekhina and Y. A. Petrovich, "Free-radical Oxidation and Antioxidant system," *Proper Economic Resource Management*, 2005, p. 69 (in Russian).

[4] A. P. Golikov, P. P. Golikov and V. B. Davydov, "Influence of Mexidol on Oxidative Stress in Cerebral Form of Hypertensic Crisis," *Kardiologiya*, Vol. 42, No. 3, 2002, pp. 25-29. (in Russian).

[5] L. A. Mansurova, O. V. Fedchishin, V. V. Trofimov, T. G. Zelenina and L. E. Smolyanko, "Physiological Role of Silicium," *Sibirskiy Meditsinskiy Zhurnal*, No. 7, 2009, pp. 16-18. (in Russian).

[6] H.-M. Shen, Z. Zhang, Q.-F. Zhang and C.-N. Ong, "Reactive Oxygen Species and Caspase Activation Mediate Silica-Induced Apoptosis in Alveolar Macrophages," *American Journal of Physiology Lung Cellular and Molecular Physiology*, Vol. 280, No. 1, 2001, pp. 10-17.

[7] E. G. Barrett, C. Johnston, G. Oberdörster and J. N. Finkelstein, "Silica-Induced Chemokine Expression in Alveolar Type Ii Cells Is Mediated by Tnf-induced Oxidant Stress," *American Journal of Physiology Lung Cellular and Molecular Physiology*, Vol. 276, No. 6, 1999, pp. 979-988.

[8] M. Ding, X. Shi, Y. J. Lu, C. Huang, S. Leonard, J. Roberts, *et al.*, "Induction of Activator Protein-1 through Reactive Oxygen Species by Crystalline Silica in JB6 Cells," *Journal of Biological Chemistry*, Vol. 276, No. 12, 2001, pp. 9108-9114.

[9] M. Ishihara, "Studies on Lipoperoxide of Normal Pregnant Women and Patient Toxemia of Pregnancy," *Clinica Chimica Acta*, Vol. 84, No. 1-2, 1978, pp. 1-9.

[10] R. Stangl, W. Platzer and V. Wittwer, "IR Emission Spectroscopy of Silica Aerogel," *Journal of Non-Crystalline Solids*, Vol. 186, 1995, pp. 256-263.

[11] M. A. S. Pedroso, M. L. Dias and C. Azuma, and C. G. Mothe, "Hydrocarbon Dispersion of Nanospherical Silica by Sol-Gel Process. 1. Tetraethoxysilane Homopolymerization," *Colloid and Polymer Science*, Vol. 278, No. 12, 2000, pp. 1180-1186.

[12] R. Urlaub, U. Posset and R. Thull, "FT-IR Spectroscopic Investigations on Sol-gel-derived Coatings from Acid-Modified Titanium Alkoxides," *Journal of Non-Crystalline Solids*, Vol. 256, 2000, pp. 276-284.

[13] R. L. Derosa and J. A. Trapasso, "Poly(Ethylene Glycol) Interactions with Alumina and Silica Powders Determined via DRIFT," *Journal of Materials Science*, Vol. 37, No. 6, 2002, pp. 1079-1082.

[14] B. Lee, Y. Kim, H. Lee and J. Yi, "Synthesis of Functionalized Porous Silicas via Templating Method as Heavy Metal Ion Adsorbents: The Introduction of Surface Hydrophilicity onto the Surface of Adsorbents," *Microporous and Mesoporous Materials*, Vol. 50, No. 1, 2001, pp. 77-90.

[15] H. S. Mansur, W. L. Vasconcelos, R. F. S. Lenza, R. L. Orefice, E. F. Reis and Z. P. Lobato, "Sol-Gel Silica Based Networks with Controlled Chemical Properties," *Journal of Non-Crystalline Solids*, Vol. 273, No. 1-3, 2000, pp. 109-115.

[16] X. Li and T. A. King, "Spectroscopic Studies of Sol-Gel-Derived Organically Modified Silicates," *Journal of Non-Crystalline Solids*, Vol. 204, No. 3, 1996, pp. 235-242.

[17] S.-H. Rhee, J.-Y. Choi and H.-M. Kim, "Preparation of a Bioactive and Degradable Poly(ε-caprolactone)/silica Hybrid through a Sol-gel Method," *Biomaterials*, Vol. 23, No. 24, 2002, pp. 4915-4921.

[18] J. Gallardo, A. Duran, D. Di Martino and R. M. Almeida, "Structure of Inorganic and Hybrid SiO_2 Sol-Gel Coatings Studied by Variable Incidence Infrared Spectros-

copy," *Journal of Non-Crystalline Solids*, Vol. 298, No. 2-3, 2002, pp. 219-225.

[19] V. A. Maroni and S. J. Epperson, "An in Situ Spectroscopic Investigation of the Pyrolysis of Ethylene Glycol Encapsulated in Silica Solidate," *Vibrational Spectroscopy*, Vol. 27, No. 1, 2001. pp. 43-51.

[20] A. I. Zhuravlev and A. I. Zhuravleva, "Hiperweak Luminescence of Blood Serum and its Role in Complex Diagnostics," Meditsina Press, Moscow, 1976. (in Russian).

[21] E. I. Kuzmina, A. S. Nelubin and M. K. Schennikova, "Application of Induced Chemiluminescence for Free-Radical Processes Estimation in Biological Substrates," In: Biokhimiya i biofizika, Gorkiy, 1983, pp. 179-183. (in Russian).

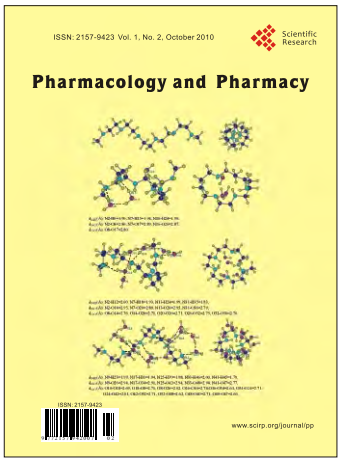

Call for Papers

Pharmacology & Pharmacy

http://www.scirp.org/journal/pp

Pharmacology & Pharmacy (PP) is a peer reviewed international journal dedicated to the latest advancement of pharmacology and pharmacy. The goal of this journal is to keep a record of the state-of-the-art research and to promote study, research and improvement within its various specialties.

Subject Coverage

The journal publishes original papers including but not limited to the following fields:

- Analytical Toxicology
- Biochemical Pharmacology
- Clinical Pharmacology
- Drug Metabolism
- Immunopharmacology
- Medicinal Chemistry and Pharmacognosy
- Molecular Pharmacology
- Neuropsychopharmacology
- Pharmaceutics
- Pharmacokinetics
- Pharmacogenetics
- Pharmacy Practice

We are also interested in short papers (letters) that clearly address a specific problem, and short survey or position papers that sketch the results or problems on a specific topic. Authors of selected short papers would be invited to write a regular paper on the same topic for future issues of the **PP**.

Notes for Intending Authors

All manuscripts submitted to PP must be previously unpublished and may not be considered for publication elsewhere at any time during PP's review period. Paper submission will be handled electronically through the website. All papers are refereed through a peer review process. Additionally, accepted ones will immediately appear online followed by printed in hard copy. For more details about the submissions, please access the website.

Website and E-Mail

http://www.scirp.org/journal/pp Email: pp@scirp.org

Pharmacology & Pharmacy, **2010, 1, 39-74**
Published Online October 2010 in SciRes (http://www.SciRP.org/journal/pp/).

TABLE OF CONTENTS

Volume 1 Number 2 **October 2010**

Colchicine-Induced Rhabdomyolysis and Possible Amiodarone Interaction

C. B. Salem, J. Sakhri, N. Fathallah, B. Trimech, H. Hmouda, B. Kamel..... 39

Rational Drug Delineation: A Global Sensitivity Approach Based on Therapeutic Tolerability to Deviations in Execution

D. G. Gohore, F. Fenneteau, O. Barrière, J. Li, F. Nekka..... 42

Antioxidant Effect of Atorvastatin in Type 2 Diabetic Patients Tablet of Diazepam-Hydroxypropyl-β-Cyclodextrin Inclusion Complex

N. R. Hadi, M. A. Abdelhussein, O. M. O. Alhamami,
A. R. M. Rudha, E. Sabah..... 53

Structure Analysis for Hydrate Models of Ethyleneimine Oligomer by Quantum Chemical Calculation

M. Kobayashi, H. Sato..... 60

The Study of Influence of Silica and Polyethilene Glycols Organic-Inorganic Compounds on Free-Radical Processes *in Vitro*

O. G. Sitnikova, S. B. Nazarov, I. V. Shikhanova,
A. V. Agafonov, J. A. Dyuzhev, I. G. Popova..... 69